

Materials and Methods

Case selection and tissue microarray construction

Study approval was obtained from the University of Pittsburgh (IRB# PRO13020493) and Washington University (201404143) Institutional Review Boards. The surgical pathology archives from the Departments of Pathology at the University of Pittsburgh Medical Center and Barnes-Jewish Hospital were queried for neuroendocrine neoplasms of the pancreas between 1995 and 2014 that underwent enucleation, central pancreatectomy, pancreaticoduodenectomy or distal pancreatectomy. Cases were cross-referenced with clinical and follow-up data obtained from patient paper and/or electronic medical records. The study inclusion criteria consisted of the following: a solitary, well-differentiated neuroendocrine tumor (confirmed with positive immunolabeling for neuroendocrine markers [e.g. synaptophysin and chromogranin A]) centered within the pancreas, surveillance and survival data of >2 years, absence of a genetic syndrome associated with pancreatic neuroendocrine neoplasms (e.g. multiple endocrine neoplasia type 1 [MEN 1] syndrome, von Hippel-Lindau [VHL] syndrome, neurofibromatosis type 1 [NF1] syndrome, and tuberous sclerosis complex [TSC] syndrome), and cases with sufficient material for ancillary studies.

In total, 367 patients with a resected PanNET fulfilled the aforementioned criteria. In addition, the surgical pathology archives from the respective institutions were cross-referenced to identify corresponding distant metastases with sufficient pathologic material for ancillary studies. Among 120 patients with distant metastases, 72 patients had pathologic material available of the distant metastasis for ancillary studies. For whole-exome sequencing, 20 distant metastatic PanNETs from 20 patients were selected

Pathologic material of the surgically resected primary PanNET from the remaining 347 patients was used to create high-density tissue microarrays (TMAs) as previously described.¹ High-density TMAs were constructed using archival FFPE tissue blocks. Three, 1.0 mm-sized cores were punched from representative areas of each patient's tumor and collected into recipient blocks. Sufficient tissue for ancillary studies on cut sections was confirmed prior to immunohistochemical testing and fluorescence in situ hybridization. Details of both whole-exome sequencing and PanNET cohorts are discussed in detail in the Supplementary Data Section.

Clinical and demographic data were reviewed for each case. Corresponding pathology gross reports and hematoxylin-and-eosin (H&E) stained slides were also reviewed for the following pathologic features: tumor size, location, lymphovascular invasion, perineural invasion, extension outside of the pancreas and regional lymph node metastasis. Each PanNET was graded using the 2010 World Health Organization (WHO) classification system for pancreatic neuroendocrine neoplasms.² Briefly, on the basis of mitotic rate and Ki-67 immunohistochemistry, the following criteria were used: Grade 1 (G1), <2 mitoses/10 high-power fields (hpf) and Ki-67 of <3%; Grade 2 (G2), 2 to 20 mitoses/10 hpf or Ki-67 of 3% to 20%; and Grade 3 (G3), >20 mitoses/10 hpf or Ki-67 of >20%. The mitotic rate was derived from evaluation of multiple sections in 50 hpf (400x, field diameter 0.55 mm²) and expressed as mitoses/10 hpf. For Ki-67, at least 500 neoplastic nuclei were counted in the highest staining region for each case with careful exclusion of non-neoplastic cells.³ A labeling index was calculated and expressed as a percentage. For cases with discordant mitotic rate and Ki-67 measurements, the highest grade was assigned. Pathologic primary tumor classification was determined according to the American Joint Committee on Cancer (AJCC) Staging Manual,

seventh edition.⁴ Follow-up information was extracted from the patient's paper and electronic medical records to include data on surveillance, disease recurrence/distant metastasis, and survival.

Whole-exome sequencing: sample and library preparation and next-generation sequencing

Whole-exome sequencing was performed in the University of Pittsburgh Cancer Institute, Cancer Genomics Facility (CGF). Ten, 5 um unstained formalin-fixed, paraffin-embedded (FFPE) sections from both tumor and normal were used sample and library preparation. Paraffin was melted in an air incubator (60°C, 30 min), removed by submerging in 100% xylene (5 min) and rinsing in 100% ethanol three times followed by centrifugation (R5810; S4-104 rotor with slide adaptor; Eppendorf, Hamburg, Germany; 1000g; 5 min). Each unstained slide was aligned in register with its corresponding H&E and the demarcated tumor or normal phenotype domain was manually dissected with a sterile scalpel with substrate accumulated across serial slides in a 2.0 mL low retention, nuclease free tube in which the substrate underwent 2 additional xylene and ethanol washes. A stereomicroscope was utilized to assist manual microdissection (Olympus SZ61 microscope, Olympus Corp., Center Valley, PA) as needed. DNA purification was performed on all samples using the QiaAmp FFPE DNA extraction kit (Qiagen, Hilden, Germany) beginning with an overnight incubation in lysis buffer (Buffer ATL: Proteinase K; 300 uL:100 uL, 56°C, shaking at 600 rpm) followed by a 100 uL proteinase spike-in and a 24 hour lysis. After the second lysis regimen, the substrate was denatured (90°C; 60 min); subjected to ethanol precipitation (2X volume and buffer AL); and QIAamp column capture was performed using a 2 mL flow-through collection tube (6000g, 1 min). The column was serially washed (buffer AW1, AW2; 6000g, 1 min) and dried (20,000g; 3 min) and the DNA eluted in low TE

buffer (53 uL Tris 10 mM;EDTA 0.1 mM, pH 8.0; 20,000g, 5 min). QA/QC analysis was performed utilizing an established pipeline including spectrophotometry for purity (NanoDrop 1000, OD 260/280 >1.8; Thermo Scientific, Grand Island, NY, USA), quantitative fluorometry for double stranded DNA yield (Qubit-High Sensitivity, >100 ng dsDNA, Thermo Scientific) and micro-capillary electrophoresis to determine DNA integrity (Bioanalyzer 2100, fragment size >500 bp, Agilent, Santa Clara, CA, USA).

The DNA samples were subjected to acoustical shearing (200ng, 50μl low TE) using a Covaris S1 (Covaris, Woburn, MA, USA) to obtain a fragment size of 150-170 bp for processing with the SureSelectXT library Prep kit (SSXT: #G9611A, Agilent). End repair was performed on individual samples (10X End Repair Buffer: 10 uL, dNTP mix: 1.6 uL, DNA polymerase: 1 uL, Klenow DNA polymerase: 2 uL, T4 Polynucleotide Kinase: 2.2 uL, nuclease free H₂O: 33.2 uL; 60 min, 20°C) and the DNA captured using Agencourt AMPure beads (#A63881; Beckman-Coulter, Indianapolis, IN) with elution in nuclear free H₂O. End-repaired DNA underwent 3' adenylation (10x Klenow Polymerase Buffer: 5 uL, dATP: 1uL, Exo (-) Klenow enzyme: 3 μl, NF H₂O: 11 μl; 37°C, 30 min) followed by AMPure bead purification. Adapters were ligated to the paired ends (5x T4 DNA Ligase Buffer: 10 uL, T4 DNA Ligase: 1.5 uL, undiluted Adaptor Oligo Mix: 10 uL, nuclease free H₂O: 15.5 uL; 20°C, 15 min) followed by AMPure bead purification and PCR amplification was performed (98°C: 2 min, 10 cycles at 98°C: 30 sec; 65°C: 30 sec; 72°C: 1 min; 72°C: 10 min) using SS primers (#G9611A) and the Herculase II Fusion DNA polymerase kit (#600679, Agilent). The DNA samples underwent QC to ensure adequate yield (>500 ng) of fragments 225 to 275 bp after PCR and AMPure bead purification.

Hybridization (SS Human All Exon V6, Agilent) was performed on individual samples (500ng DNA: 3.4 uL, SureSelect Block: 5.6 uL) which were then denatured at 95°C prior to

mixing with capture baits (hyb buffer: 13 uL, baits: 5 uL, RNase Block: 2 uL; 65°C, 24hrs). Hybridization products were then captured by incubation with streptavidin T1 beads (Dynabeads MyOne Streptavidin T1, Thermo Fisher, Waltham, MA, USA) in SS binding buffer (room temp, 30 min) followed by separation in a magnetic rack. Beads were washed (SS wash 2, 200 uL, 65°C, 10 min) and resuspended in H₂O followed by amplification with indexing primers (Illumina, San Diego, CA, USA) generating unique bar codes for each sample (H₂O: 18.5 uL, 5X Herculase II reaction buffer: 10 uL, 100 mM dNTP: 0.5 uL, Herculase polymerase: 1uL, indexing post-capture PCR primer: SSXT Index Reverse primers: 5 uL, DNA: 14 uL; 98°C: 2 min; 11 cycles 98°C: 30 sec; 57°C: 30 sec; 72°C: 1 min). The DNA library was recovered using AMPure beads. Sequencing was performed using the NextSeq 500 (Illumina, San Diego, CA, USA) high output flow cell kit (2 x 76 paired end, 150 cycles) with samples concentrated (660 g/mol X bp fragment size x 1X10⁶), pooled and titrated to 1.7 pM per sample to achieve an average base call target depth of 63x to 102x.

Sequencing data processing and variant detection

Bioinformatics analysis was performed using a custom protocol developed for tumor and paired normal analysis. First, base call (BCL) files were converted to FASTQ files using bcltofastq (Illumina, San Diego, CA, USA). Per lane FASTQ files were merged into FASTQ files for each read pair (R1 & R2), as per manufacturer's recommendation. Each set of read pair FASTQs were aligned to the human reference genome (GRCh37.p13, hg19; GCF_000001405.25) using BWA MEM and encoded into a BAM (binary sequence alignment) format using Samtools.^{5, 6} RG (read group) tags for each sample were added at the time of sequence alignment. The raw BAM files were sorted, indexed and PCR duplicates marked using

Sambamba.⁷ Pre-variant calling processing included concurrent local realignment around regions of known indels (COSMIC v80, dbSNPv138 and Mills gold-standard indel sets) for both tumor and normal aligned reads using GATK.⁸⁻¹⁰ Subsequently, realigned BAMs were subjected to BQSR (Base Quality Score Recalibration) using GATK. Subsequently, variant calling was performed on the recalibrated BAMs using Varscan2 for SNV and short Indel detection and Scalpel for larger Indel detection.^{11, 12} Briefly for Varscan2, recalibrated BAM files for both tumor and normal were used to generate a paired tumor-normal sequence mpileup, which was used for calling variants using Varscan2 in somatic mode. Potential false positives were marked in the VCF files using Varscan2's fpfilter based on specific parameters. Variants marked as somatic and high confidence by the variant caller were prioritized. For large indel detection, Scalpel was used in somatic (paired tumor-normal) mode. Variants were represented using VCF format v4.2 (<https://samtools.github.io/hts-specs/VCFv4.2.pdf>). Variant calls from both callers were integrated, normalized and annotated using custom python modules with dependencies on ANNOVAR and HGVS python package.^{13, 14} For FASTQ and BAM files, quality control (QC) metrics were generated by FastQC (<http://www.bioinformatics.babraham.ac.uk/projects/fastqc/>) and QualiMap, respectively.¹⁵ For variant calling, sequence reads with minimum base quality score (Phred score) of 30 and minimum mapping quality score of 20 were used. Integrative Genomics Viewer (IGV, Broad Institute) was used for manual review of sequence pileups and detected variants.¹⁶ Genomic data was visualized and reviewed using custom developed javascript plugin, jsComut (<https://github.com/pearcetm/jscomut>).

Gene and variant prioritization

Variants and genes were prioritized following the 2017 AMP/ASCO/CAP joint consensus guidelines for interpretation of sequence variants in cancer.¹⁷ Briefly, variants that were present at a minor allele frequency greater than or equal to 1% in population databases (1000genomes, ExAC-nonTCGA and Exome server variant) were filtered out as benign/likely benign.¹⁸⁻²⁰ Subsequently, non-coding variants in deep intronic, intergenic and untranslated regions, and missense variants with benign/tolerated in silico predictions (SIFT and PolyPhen2) were also filtered out.^{21, 22} Truncating variants that introduced premature stop codon (frameshift deletions and insertions, stop gain and splice site) in genes where loss of function is associated with oncogenesis, were prioritized as tier I/II and included for analysis. Similarly, missense and inframe indels in genes where gain of function is implicated in oncogenesis were prioritized as Tier I/II variants based on incidence in public somatic mutation databases (COSMIC v80 and TCGA), review of gene specific published functional studies, and damaging/deleterious in silico predictions.^{17, 23} Germline mutation database (ClinVar) was also reviewed for prioritization of a subset of variants.²⁴ Unless supporting data for pathogenicity was available from published literature or public databases, Tier III variants (variants of uncertain clinical significance) were not prioritized.¹⁷

Copy number variation analysis

Copy number analysis was performed using Nexus Biodiscovery software (version 8.1, El Segundo, CA) designed to take into consideration the significant mosaicism, hyperploidy and normal cell heterogeneity that is present in cancer samples even after microdissection to enrich for tumor cells. Match paired next-generation sequencing analysis required 2 BAM files comprising the tumor and normal sequence for each specimen which were combined into one

result via subtraction of the \log_2 ratios revealing copy number changes specific to the tumor sample. The GISTIC algorithm was used to identify aggregate regions with a statistically high frequency of copy number aberrations (gains and losses) from the global data set.²⁵ This method applies FDR (false discovery rate) correction for multiple testing and computes the Q-bound values (Q-Bound cutoff = 0.05, G-Score cut-off = 1.0). Individual gene queries employed the STAC (Significance testing for Aberrant Copy Number) algorithm using a minimum of 1000 reference reads per segment and the Nexus FASST2 (Fast Adaptive States Segmentation Technique) Segmentation algorithm with significance value = 1×10^{-6} .²⁶

In addition, CNVKit (0.8.6.dev) was used as an alternate method to assess copy number changes from whole exome sequencing.²⁷ Briefly, a pool of normal reference was created using the aligned sequences from the paired normal samples. Subsequently, target and anti-target regions were created using the SureSelect exome v6 BED file. Next, the binned coverage for each of the loci in the target and the anti-target regions were computed. The binned coverage from the pool of normal reference was then used to normalize each tumor sample and correct biases (e.g. GC bias). Finally, copy number ratios were calculated and segmented using circular binary segmentation. Copy number changes were assessed manually using scatter plot visualization provided by CNVKit and compared to the calls made by the Nexus Biodiscovery software.

Immunohistochemistry

TMA slides were cut at 4-um and deparaffinized with serial xylene treatments and subjected to antigen retrieval using heated citrate solution (pH 9.0) at 100°C for 10 minutes. Immunolabeling for Ki-67 (mouse monoclonal, prediluted, Ventana Medical Systems, Tucson,

AZ, USA), synaptophysin (rabbit polyclonal, prediluted, Cell Marque, Rocklin, CA, USA), chromogranin A (mouse monoclonal, prediluted, Ventana Medical Systems, Tucson, AZ, USA), DAXX (HPA008736 rabbit polyclonal, dilution 1:50, Sigma Aldrich, St Louis, MO, USA) and ATRX (HPA001906 rabbit polyclonal, dilution 1:100, Sigma Aldrich, St Louis, MO, USA), H3K36me3 (AB9050 rabbit polyclonal, dilution 1:1000, Abcam, Eugene, OR, USA), and ARID1A (AB182560 rabbit monoclonal, dilution 1:1000, Abcam, Eugene, OR, USA) were performed on the automated Ventana Benchmark XT system using the biotin-free Ventana OptiView DAB IHC Detection Kit (Ventana Medical Systems, Tucson, AZ, USA).

Assessment of DAXX, ATRX, H3K36me3 and ARID1A was done blinded to any patient data including outcome. Preserved or “positive” expression was defined as nuclear staining within tumor cells; using stromal cells as a positive internal control. Loss or “negative” staining was scored in cases where the tumor lacked nuclear immunolabeling, but preserved expression within stromal cells was still identified. Intratumoral heterogeneity or heterogeneous staining was defined as the clear presence of two distinct populations of tumor cells demonstrating preserved and loss of nuclear staining. For cases with heterogeneous staining, each component (positive or preserved and negative or loss of nuclear staining) should comprise at least 10% of the neoplastic tissue.¹ For subsequent statistical analysis, these cases were scored as loss or negative staining.

Fluorescence in situ hybridization

Telomere-specific FISH was performed as previously described using an Alexa-488 telomeric-C PNA probe.¹ In brief, 4-um TMA sections were incubated for 30 min at 55°C, washed three times for 5 min in xylene, rinsed in successive 100%, 95%, and 70% ethanol baths,

and washed in double-distilled H₂O and 1% Tween before being placed in antigen unmasking solution in a boiling steamer for 30 min. Next, slides were rinsed in double-distilled H₂O and dehydrated in successive ethanol washes of 70%, 95%, and 100%. Slides were incubated at 72°C for 10 min with an Alexa-488 telomeric-C PNA probe and hybridized overnight in a dark humidity chamber. Slides were washed with PNA wash buffer and PBST and incubated for 10 min in DAPI solution. After washing in double-distilled H₂O, slides were mounted with prolong anti-fade mounting medium. Images were taken on a Leica fluorescent light microscope.²⁸

Scoring for ALT was performed by assessing at least 250 nuclei from all 3 tissue cores for each case (at least 750 tumor nuclei). Using previously described criteria, ALT-positive cases were defined by the presence of large, ultrabright intranuclear foci consistent with telomere FISH signals in at least 1% of tumor nuclei and the total signal intensity for individual foci >10 fold than telomere signals from stromal cells. Of note, areas of necrosis were excluded from evaluation. Among ALT-negative PanNETs, no large, ultrabright, intranuclear signals were found in over 750 tumor nuclei that were screened.

Dual color fluorescence *in situ* hybridization was performed for *CDKN2A* within a Clinical Laboratory Improvement Amendments (CLIA)-accredited and College of American Pathologist (CAP)-approved laboratory as previously reported.²⁹ *CDKN2A* was assessed using a Spectrum-Orange labeled, locus-specific probe (Abbott Molecular, Des Plains, IL, USA) with a Spectrum Green-labeled chromosome 9 centromeric (CEP9) probe. Scoring of *CDKN2A* FISH was performed on only individual and well-delineated cells; overlapping cells were excluded from the analysis. At least 60 cells were scored for each case and controls. Each tumor was assessed by the average and the maximum numbers of copies of p16 gene per cell and the average ratio of p16 gene to chromosome 9 copy numbers (CEP9). Deletion was defined if both

CDKN2A signals were lost in at least 20% of nuclei and showed at least one signal for the CEP9 probe.

Statistical analysis

Chi-squared analysis or Fisher exact tests were used to compare categorical data, and analysis of variance was used to compare continuous variables. Survival curves were constructed using the Kaplan-Meier method and differences between groups were evaluated by the log-rank test. Disease-free survival (DFS) was calculated from the date of surgery to the date of first distant metastasis/recurrence after surgery or to the date of last follow-up (in patients without distant metastasis/recurrence) for cases without synchronous distant metastasis. Disease-specific survival (DSS) was calculated from the date of surgery to the date of death due to disease or date of last follow-up (if death did not occur). The prognostic significance of clinical and pathologic characteristics was determined using univariate Cox regression analysis. Multivariate analyses of significant risk factors by univariate analysis were performed using Cox proportional hazard regression to identify independent risk factors for both DFS and DSS. All statistical analyses were performed using the SPSS Statistical software, version 24 (IBM, Armonk, NY) and statistical significance was defined as a p value of < 0.05.

Supplementary Data

Distant metastatic PanNET whole-exome sequencing cohort

The whole-exome sequencing cohort consisted of 20 distant metastases from 20 patients with a solitary, non-syndromic PanNET. At initial presentation, patients ranged in age from 42 to 80 years (mean, 55.1 years) and included 11 females and 9 males. The patients' corresponding primary tumors were treated by either pancreaticoduodenectomy ($n = 10$) or distal pancreatectomy ($n = 10$) and pathologically confirmed to be of pancreatic origin. The primary PanNETs were distributed within the pancreas as follows: 10 in the head, 7 in the tail and 3 in the body; and ranged in size from 2.5 to 18 cm (mean, 6.2 cm). None of the PanNETs were biochemically functional.

The metastatic PanNETs consisted of 9 synchronous and 11 metachronous distant metastases, which were surgically resected from the liver ($n = 19$) or remnant pancreas ($n = 1$). Among the metachronous distant metastases, the time interval between pancreaticoduodenectomy or distal pancreatectomy and metastasectomy ranged between 1.7 to 7.8 years (mean, 4.5 years). Prior to metastatectomy, 6 of 20 (30%) patients received chemotherapy ($n = 5$) and/or underwent transarterial chemoembolization (TACE) to the liver ($n = 2$, MetaPanNET-7 and -17). All 6 patients presented with metachronous metastases. Among 5 patients that received chemotherapy, 3 patients received octreotide (MetaPanNET-10, -17 and -19) and 1 patient received everolimus (MetaPanNET-19). MetaPanNET-5 received multiple regimens of chemotherapy that included cisplatin and etoposide, carboplatin and etoposide, and irinotecan hydrochloride. Although neoadjuvant chemotherapy was documented for MetaPanNET-13, the exact regimen the patient received is unknown. While all metastatic PanNETs were morphologically well-differentiated, on the basis of mitotic rate and Ki-67

proliferation index, the tumors were classified into the following WHO grades: 1 (5%) grade 1 (G1), 13 (65%) grade 2 (G2), and 6 (30%) grade 3 (G3). Telomere-specific FISH identified ALT in 12 (60%) metastatic PanNETs and loss of nuclear expression for DAXX, ATRX or both proteins was seen in 4 (20%), 4 (20%), and 3 (15%) cases, respectively. One (5%) ALT-positive PanNET had preserved expression for DAXX/ATRX.

Primary PanNET study cohort

The study cohort consisted of 347 patients with a solitary PanNET treated by enucleation ($n = 14$), central pancreatectomy ($n = 15$), pancreaticoduodenectomy ($n = 131$) or distal pancreatectomy ($n = 187$) to include resection of identifiable metastases with curative intent. None of the patients received neoadjuvant chemotherapy, radiation or chemoembolization prior to surgical intervention. Patients ranged in age from 26 to 85 years (mean, 59 years) with a slight predominance in male gender (181 of 347, 52%). Thirty-six of 347 (10%) patients had a functional PanNET and included: 21 insulinomas, 8 gastrinomas, 5 glucagonomas, 1 somatostatinoma, 1 VIPoma and 1 ACTH-producing PanNET. The tumors were predominantly located within the pancreatic body and tail ($n = 216$, 62%) and ranged in size from 0.6 to 18 cm (mean, 3.4 cm). All PanNETs were morphologically well-differentiated, and, on the basis of mitotic rate and Ki-67 proliferation index, these tumors were classified into the following WHO grades: 199 (57%) grade 1 (G1), 140 (40%) grade 2 (G2), and 8 (3%) grade 3 (G3). Lymphovascular and perineural invasion were identified in 153 (44%) and 91 (26%) tumors, respectively. Using the AJCC prognostic staging system (seventh edition), the PanNETs were classified into the following pathologic tumor (pT) stages: 121 (35%) pT1, 106 (30%) pT2, and 120 (35%) pT3. Regional lymph nodes were submitted for histologic evaluation in 294 (85%)

cases with involvement of 110 (of 294, 37%) cases. At the time of surgery, 54 (16%) patients were found to have synchronous distant metastases that were resected. Of the remaining 292 patients, metachronous distant metastases were identified in 45 (of 292, 15%) cases. The DFS rates for these 292 patients were 91% at 3 years and 83% at 5 years. For all 347 patients, the DSS rates were 90% at 5 years and 76% at 10 years.

Immunohistochemistry for DAXX and ATRX and telomere-specific FISH were performed for all 347 PanNETs. Loss of nuclear expression for DAXX, ATRX, or both was identified in 37 (11%), 29 (8%), and 14 (4%) PanNETs, respectively. Of note, among the DAXX/ATRX-negative cases, heterogeneous loss of expression was seen in 1 DAXX-negative and 3 ATRX-negative PanNETs.¹ For these cases, the number of neoplastic nuclei lacking staining for DAXX/ATRX ranged between 65% to 80%. In addition, 94 (27%) PanNETs demonstrated large, ultrabright intranuclear foci consistent with ALT. The presence of ALT correlated with DAXX/ATRX loss ($p < 0.001$), but 14 (4%) ALT-positive PanNETs had preserved expression for DAXX/ATRX. Similar to DAXX and ATRX, heterogeneous loss of expression was seen in 1 of 28 H3K36me3-negative PanNETs with lack of staining in 80% of the neoplastic nuclei, while all 10 ARID1A-negative PanNETs exhibited complete loss of nuclear expression for ARID1A.

Patients with PanNETs exhibiting loss of DAXX/ATRX, H3K36me3, or deletion in *CDKN2A* were associated with shorter DFS; while, patients with PanNETs showing loss of DAXX/ATRX, H3K36me3, ARID1A or deletion in *CDKN2A* were associated with poor DSS (Supplementary Figure 3). Disease-free survival (DFS) rates for patients with DAXX/ATRX-negative (loss of DAXX/ATRX) PanNETs were 60% at 3 years and 40% at 5 years ($p < 0.001$, $\chi^2 = 96.5$), H3K36me3-negative PanNETs were 86% at 3 years and 11% at 5 years ($p < 0.001$,

$X^2 = 28.3$), ARID1A-negative PanNETs were 80% at 3 years and 60% at 5 years ($p = 0.221$, $X^2 = 1.50$), and *CDKN2A*-negative PanNETs were 53% at 3 years and 38% at 5 years ($p < 0.001$, $X^2 = 50.2$). In comparison, DSS rates for patients with DAXX/ATRX-negative PanNETs were 78% at 5 years and 48% at 10 years ($p < 0.001$, $X^2 = 21.5$), H3K36me3-negative PanNETs were 71% at 5 years and 34% at 10 years ($p < 0.001$, $X^2 = 13.9$), ARID1A-negative PanNETs were 80% at 5 years and 27% at 10 years ($p < 0.001$, $X^2 = 13.6$), and *CDKN2A*-negative PanNETs were 69% at 5 years and 35% at 10 years ($p < 0.001$, $X^2 = 18.8$).

Results of Cox regression analysis for DFS and DSS in relationship to various clinicopathologic features is presented in Table 1. By univariate Cox regression analysis, shorter DFS and poor DSS were associated with age ($p = 0.008$ and $p = 0.038$, respectively), tumor size > 2.0 cm ($p < 0.001$ and $p = 0.001$), G2-to-G3 WHO grade ($p < 0.001$ and $p < 0.001$, respectively), lymphovascular invasion ($p < 0.001$ and $p < 0.001$), perineural invasion ($p < 0.001$ and $p < 0.001$), advanced tumor stage ($p < 0.001$ and $p < 0.001$) and regional lymph node (pN) metastasis ($p < 0.001$ and $p < 0.001$). A separate univariate analysis was performed for DAXX/ATRX and H3K36me3/ARID1A/*CDKN2A* status, independently. Loss of DAXX/ATRX and loss/deletion of H3K36me3/ARID1A/*CDKN2A* were associated with shorter DFS (HR = 12.08 [95% CI, 6.42 – 22.75], $p < 0.001$; HR = 9.07 [95% CI, 4.99 – 16.49] , $p < 0.001$, respectively) and poor DSS (HR = 3.67 [95% CI, 2.04 – 6.61], $p < 0.001$; HR = 6.35 [95% CI, 3.52 – 11.48], $p < 0.001$, respectively). Multivariate analysis was used to determine the prognostic significance of H3K36me3/ARID1A/*CDKN2A* status for DFS and DSS and included tumor size > 2.0 cm, WHO grade, regional lymph node metastasis and DAXX/ATRX loss. Independent prognostic factors for shorter DFS included tumor size > 2.0 cm (HR = 17.08 [95% CI, 2.31 – 126.40], $p = 0.005$), regional lymph node metastasis (HR = 2.03 [95% CI, 1.05 –

3.90], $p = 0.034$), DAXX/ATRX loss (HR = 4.64 [95% CI, 2.39 – 9.04], $p < 0.001$) and H3K36me3/ARID1A/CDKN2A loss/deletion (HR = 3.63 [95% CI, 1.93 – 6.81], $p < 0.001$). In comparison, independent prognostic factors for poor DSS included tumor size > 2.0 cm (HR = 9.47 [95% CI, 1.29 – 69.56], $p = 0.027$), G2-to-G3 WHO grade (HR = 2.29 [95% CI, 1.09 – 4.78], $p = 0.028$), regional lymph node metastasis (HR = 2.30 [95% CI, 1.14 – 4.65], $p = 0.020$) and H3K36me3/ARID1A/CDKN2A loss/deletion (HR = 3.07 [95% CI, 1.65 – 5.68], $p < 0.001$). Consistent with our prior study, DAXX/ATRX loss was not an independent prognostic factor for DSS.¹

Acknowledgements

The authors would like to thank Mrs. Kate Smith for outstanding administrative assistance. We also thank Siraj Ali, MD from Foundation Medicine, Inc. for sharing unpublished data. This study was supported in part by a grant from the National Pancreas Foundation, Western Pennsylvania Chapter (to A. D. Singhi). This project utilized the University of Pittsburgh Cancer Institute shared resource facility (Cancer Genomics Facility) supported in part by award P30CA047904 (to W. A. LaFramboise).

Supplementary Figure Legends

Supplementary Figure 1. Key genomic alterations identified in 20 metastatic pancreatic neuroendocrine tumors (PanNETs). (A) Each metastatic PanNET was classified based on World Health Organization (WHO) grade, timing of metastasis (synchronous versus metachronous with respect to the patient's primary PanNET), and ATRX and DAXX immunohistochemistry, and telomere-specific fluorescence *in situ* hybridization for alternative lengthening of telomeres (ALT). These findings were correlated with recurrent genomic alterations identified by whole-exome sequencing and compared to those previously published by Scarpa et al.³⁰ Somatic mutations and copy number variation are colored according to functional class. Copy number variation analysis was performed using the Nexus Biosdiscovery software (version 8.1, El Segundo, CA) and CNVKit (0.8.6.dev) comparing matched pairs of metastatic PanNETs and normal controls. (B) Recurrent copy number loss was identified within the genomic locus that includes *CDKN2A*. An example of a metastatic PanNET (MetaPanNET-3) with copy number loss at the 9p21 locus (gray dots) and a deep deletion present in *CDKN2A* (red dots).

Supplementary Figure 2. Representative examples of pancreatic neuroendocrine tumors (PanNETs) evaluated for H3K36me3 and ARID1A by immunohistochemistry and *CDKN2A* (orange) by dual-color fluorescence *in situ* hybridization (chromosome 9, green). (A) PanNET with preserved nuclear expression for both H3K36me3 (B) and ARID1A (C), and homozygous deletion of *CDKN2A* (D, loss of both orange signals, but retention of at least one green signal; white arrow, highlights a *CDKN2A* wild type stromal fibroblast). (E) PanNET with H3K36me3 loss (F), but preserved expression for ARID1A (G) and wild type *CDKN2A* (H). (I) PanNET with ARID1A loss (K), but preserved expression for H3K36me3 (J) and wild type *CDKN2A* (L).

Supplementary Figure 3. Kaplan-Meier curves comparing the cumulative probabilities of disease-free survival (DFS) and disease-specific survival (DSS) after surgical resection among 282 patients (without synchronous distant metastases) and 347 patients with PanNETs, respectively, for DAXX/ATRX, H3K36me3, ARID1A and *CDKN2A* status. Patients with PanNETs harboring loss or deletion of DAXX/ATRX, H3K36me3 or *CDKN2A* were associated with reduced time of DFS (A, B and D); while, loss or deletion of DAXX/ATRX, H3K36me3, ARID1A or *CDKN2A* was associated with reduced time of DSS (E, F, G and H), as compared to patients with wild type PanNETs.

References

1. Singhi AD, Liu TC, Ronaioli JL, et al. Alternative Lengthening of Telomeres and Loss of DAXX/ATRX Expression Predicts Metastatic Disease and Poor Survival in Patients with Pancreatic Neuroendocrine Tumors. *Clin Cancer Res* 2017;23:600-609.
2. Bosman FT, Carneiro F, Hruban RH, et al. World Health Organization (WHO) Classification of Tumours of the Digestive System. Lyon, France: IARC Press, 2010.
3. Reid MD, Bagci P, Ohike N, et al. Calculation of the Ki67 index in pancreatic neuroendocrine tumors: a comparative analysis of four counting methodologies. *Mod Pathol* 2015;28:686-94.
4. Edge SB, Byrd DR, Compton CC, et al. Exocrine and endocrine pancreas. *AJCC Cancer Staging Manual*. 7th ed. New York, NY: Springer, 2010:241-9.
5. Li H. Aligning sequence reads, clone sequences and assembly contigs with BWA-MEM, 2013.
6. Li H, Handsaker B, Wysoker A, et al. The Sequence Alignment/Map format and SAMtools. *Bioinformatics* 2009;25:2078-9.
7. Tarasov A, Vilella AJ, Cuppen E, et al. Sambamba: fast processing of NGS alignment formats. *Bioinformatics* 2015;31:2032-4.
8. Forbes SA, Beare D, Gunasekaran P, et al. COSMIC: exploring the world's knowledge of somatic mutations in human cancer. *Nucleic Acids Res* 2014;43:D805-11.
9. Sherry ST, Ward MH, Kholodov M, et al. dbSNP: the NCBI database of genetic variation. *Nucleic Acids Res* 2000;29:308-11.

10. McKenna A, Hanna M, Banks E, et al. The Genome Analysis Toolkit: a MapReduce framework for analyzing next-generation DNA sequencing data. *Genome Res* 2010;20:1297-303.
11. Koboldt DC, Zhang Q, Larson DE, et al. VarScan 2: somatic mutation and copy number alteration discovery in cancer by exome sequencing. *Genome Res* 2012;22:568-76.
12. Fang H, Bergmann EA, Arora K, et al. Indel variant analysis of short-read sequencing data with Scalpel. *Nat Protoc* 2016;11:2529-2548.
13. Wang K, Li M, Hakonarson H. ANNOVAR: functional annotation of genetic variants from high-throughput sequencing data. *Nucleic Acids Res* 2010;38:e164.
14. Hart RK, Rico R, Hare E, et al. A Python package for parsing, validating, mapping and formatting sequence variants using HGVS nomenclature. *Bioinformatics* 2014;31:268-70.
15. Okonechnikov K, Conesa A, Garcia-Alcalde F. Qualimap 2: advanced multi-sample quality control for high-throughput sequencing data. *Bioinformatics* 2015;32:292-4.
16. Thorvaldsdottir H, Robinson JT, Mesirov JP. Integrative Genomics Viewer (IGV): high-performance genomics data visualization and exploration. *Brief Bioinform* 2012;14:178-92.
17. Li MM, Datto M, Duncavage EJ, et al. Standards and Guidelines for the Interpretation and Reporting of Sequence Variants in Cancer: A Joint Consensus Recommendation of the Association for Molecular Pathology, American Society of Clinical Oncology, and College of American Pathologists. *J Mol Diagn* 2017;19:4-23.
18. Auton A, Brooks LD, Durbin RM, et al. A global reference for human genetic variation. *Nature* 2015;526:68-74.

19. Lek M, Karczewski KJ, Minikel EV, et al. Analysis of protein-coding genetic variation in 60,706 humans. *Nature* 2016;536:285-91.
20. NHLBI Exome Sequencing Project (ESP) Exome Variant Server. Volume 2017.
21. Ng PC, Henikoff S. SIFT: Predicting amino acid changes that affect protein function. *Nucleic Acids Res* 2003;31:3812-4.
22. Adzhubei I, Jordan DM, Sunyaev SR. Predicting functional effect of human missense mutations using PolyPhen-2. *Curr Protoc Hum Genet* 2013;Chapter 7:Unit7.20.
23. Forbes SA, Beare D, Gunasekaran P, et al. COSMIC: exploring the world's knowledge of somatic mutations in human cancer. *Nucleic Acids Res* 2015;43:D805-11.
24. Landrum MJ, Lee JM, Riley GR, et al. ClinVar: public archive of relationships among sequence variation and human phenotype. *Nucleic Acids Res* 2014;42:D980-5.
25. Beroukhim R, Getz G, Nghiemphu L, et al. Assessing the significance of chromosomal aberrations in cancer: methodology and application to glioma. *Proc Natl Acad Sci U S A* 2007;104:20007-12.
26. Diskin SJ, Eck T, Greshock J, et al. STAC: A method for testing the significance of DNA copy number aberrations across multiple array-CGH experiments. *Genome Res* 2006;16:1149-58.
27. Talevich E, Shain AH, Botton T, et al. CNVkit: Genome-Wide Copy Number Detection and Visualization from Targeted DNA Sequencing. *PLoS Comput Biol* 2016;12:e1004873.
28. Cesare AJ, Heaphy CM, O'Sullivan RJ. Visualization of Telomere Integrity and Function In Vitro and In Vivo Using Immunofluorescence Techniques. *Curr Protoc Cytom* 2015;73:12 40 1-31.

29. Singhi AD, Krasinskas AM, Choudry HA, et al. The prognostic significance of BAP1, NF2, and CDKN2A in malignant peritoneal mesothelioma. *Mod Pathol* 2016;29:14-24.
30. Scarpa A, Chang DK, Nones K, et al. Whole-genome landscape of pancreatic neuroendocrine tumours. *Nature* 2017;543:65-71.

4:39851241:TC:T	MetaPanNET-14 PD55A	P055A:NM_001100998:exon27:c.3117delG:p.M1039fs
17:44617094:A:C	MetaPanNET-12 GGT6	GGT6:NM_153338:exon3:c.T992G:p.L31R x3bGGT6:NM_001122890:exon4:c.T1088G:p.L363R x3bGGT6:NM_001288702:exon4:c.T1106G:p.L369R
16:2284604:CA	MetaPanNET-20 E4F1	E4F1:NM_001288776:exon11:c.C1614A:p.F538L x3bE4F1:NM_004424:exon11:c.C1614A:p.F538L
6:29054663:G:T	MetaPanNET-2 OR2B3	OR2B3:NM_0011005226:exon1:c.C363A:p.D121E
3:195508667:T:C	MetaPanNET-1 MUC4	MUC4:NM_018406:exon2:c.G974G:p.T3262A
7:100646952:G:C	MetaPanNET-10 MUC12	MUC12:NM_001164462:exon2:c.G13108C:p.A4370P
11:31703530:T:C	MetaPanNET-14 ELPA	ELPA:NM_001288726:exon10:c.T1339C:p.S447P
14:2189795:T:C	MetaPanNET-5 CHD8	CHD8:NM_001170629:exon1:c.A8G:p.D36
1:28169731:G:A	MetaPanNET-14 PPP1R8	PPP1R8:NM_001410:exon5:c.G527A:p.R176Q x3bPPP1R8:NM_138558:exon5:c.G101A:p.R34Q
1:27107161:CTG:C	MetaPanNET-14 ARID1A	ARID1A:NM_006015:exon20:c.6773_6774del:p.L2558 x3bARID1A:NM_139135:exon20:c.D122_6123del:p.L2041fs
11:128839196:G:C	MetaPanNET-5 ARHGPAP32	ARHGPAP32:NM_0014715:exon13:c.C4823G:p.S1608Q x3bARHGPAP32:NM_001142685:exon22:c.C5870G:p.S1957C
13:42874862:G:T	MetaPanNET-5 AKAP11	AKAP11:NM_016248:exon8:c.G1980T:p.M660I
3:10413630:G:A	MetaPanNET-14 ATP2B2	ATP2B2:NM_001683:exon9:c.C1387T:p.R463C x3bATP2B2:NM_001001331:exon12:c.C1522T:p.R508C
1:181767512:G:A	MetaPanNET-17 CACNA1E	CACNA1E:NM_001205294:exon46:c.G6298A:p.V2100 x3bCACNA1E:NM_000721:exon47:c.G6355A:p.V2119 x3bCACNA1E:NM_001205293:exon48:c.G6484A:p.V2162I
16:23093835:C:T	MetaPanNET-2 USP31	USP31:NM_020718:exon12:c.G1586P:p.C619Y
14:24769849:AGAG	MetaPanNET-20 NOP9	NOP9:NM_001286367:exon2:c.483_484insGAG:p.A161delinsAE x3bNOP9:NM_174913:exon2:c.483_484insGAG:p.A161delinsAE
3:50220158:G:A	MetaPanNET-4 SEMA3F	SEMA3F:NM_004186:exon9:c.G845A:p.R282Q
X:47102994:CT	MetaPanNET-2 USP11	USP11:NM_004651:exon13:c.C1912T:p.R638W
16:11836430:G:A	MetaPanNET-13 TNNDC11	TNNDC11:NM_001303447:exon1:c.C157T:p.R53C x3bTNNDC11:NM_015914:exon1:c.C157T:p.R53C
2:25037333:A:T	MetaPanNET-2 CENPO	CENPO:NM_001199803:exon3:c.A287T:p.K96I x3bCENPO:NM_024322:exon4:c.A305T:p.K102I
7:23545827:G:C	MetaPanNET-8 TRA2A	TRA2A:NM_011293:exon3:c.C700G:p.R234G x3bTRA2A:NM_001282757:exon7:c.C397G:p.R133G x3bTRA2A:NM_001282758:exon7:c.C397G:p.R133G x3bTRA2A:NM_00128
22:36697689:C:T	MetaPanNET-17 MYH9	MYH9:NM_002473:exon21:c.G2522A:p.S841N
17:16326860:C:A	MetaPanNET-5 TRPV2	TRPV2:NM_016113:exon5:c.T703A:p.P235T
2:98162173:G:A	MetaPanNET-2 ANKRD36B	ANKRD36B:NM_025190:exon24:c.C1637T:p.P546L
9:75263571:CA	MetaPanNET-14 TMCI	TMCI:NM_138691:exon5:c.C7A:p.P37
6:97578823:C:G	MetaPanNET-6 KHL32	KHL32:NM_01286251:exon7:c.C397G:p.T466S x3bKHL32:NM_001286254:exon7:c.C212G:p.T715 x3bKHL32:NM_001286250:exon8:c.C1496G:p.T499S x3bKHL32:NM_001286256:exon9:c.C1496G:p.T499S x3bKHL32:NM_001286257:exon10:c.C1496G:p.T499S x3bKHL32:NM_001286258:exon11:c.C1496G:p.T499S x3bKHL32:NM_001286259:exon12:c.C1496G:p.T499S x3bKHL32:NM_001286260:exon13:c.C1496G:p.T499S x3bKHL32:NM_001286261:exon14:c.C1496G:p.T499S x3bKHL32:NM_001286262:exon15:c.C1496G:p.T499S x3bKHL32:NM_001286263:exon16:c.C1496G:p.T499S x3bKHL32:NM_001286264:exon17:c.C1496G:p.T499S x3bKHL32:NM_001286265:exon18:c.C1496G:p.T499S x3bKHL32:NM_001286266:exon19:c.C1496G:p.T499S x3bKHL32:NM_001286267:exon20:c.C1496G:p.T499S x3bKHL32:NM_001286268:exon21:c.C1496G:p.T499S x3bKHL32:NM_001286269:exon22:c.C1496G:p.T499S x3bKHL32:NM_001286270:exon23:c.C1496G:p.T499S x3bKHL32:NM_001286271:exon24:c.C1496G:p.T499S x3bKHL32:NM_001286272:exon25:c.C1496G:p.T499S x3bKHL32:NM_001286273:exon26:c.C1496G:p.T499S x3bKHL32:NM_001286274:exon27:c.C1496G:p.T499S x3bKHL32:NM_001286275:exon28:c.C1496G:p.T499S x3bKHL32:NM_001286276:exon29:c.C1496G:p.T499S x3bKHL32:NM_001286277:exon30:c.C1496G:p.T499S x3bKHL32:NM_001286278:exon31:c.C1496G:p.T499S x3bKHL32:NM_001286279:exon32:c.C1496G:p.T499S x3bKHL32:NM_001286280:exon33:c.C1496G:p.T499S x3bKHL32:NM_001286281:exon34:c.C1496G:p.T499S x3bKHL32:NM_001286282:exon35:c.C1496G:p.T499S x3bKHL32:NM_001286283:exon36:c.C1496G:p.T499S x3bKHL32:NM_001286284:exon37:c.C1496G:p.T499S x3bKHL32:NM_001286285:exon38:c.C1496G:p.T499S x3bKHL32:NM_001286286:exon39:c.C1496G:p.T499S x3bKHL32:NM_001286287:exon40:c.C1496G:p.T499S x3bKHL32:NM_001286288:exon41:c.C1496G:p.T499S x3bKHL32:NM_001286289:exon42:c.C1496G:p.T499S x3bKHL32:NM_001286290:exon43:c.C1496G:p.T499S x3bKHL32:NM_001286291:exon44:c.C1496G:p.T499S x3bKHL32:NM_001286292:exon45:c.C1496G:p.T499S x3bKHL32:NM_001286293:exon46:c.C1496G:p.T499S x3bKHL32:NM_001286294:exon47:c.C1496G:p.T499S x3bKHL32:NM_001286295:exon48:c.C1496G:p.T499S x3bKHL32:NM_001286296:exon49:c.C1496G:p.T499S x3bKHL32:NM_001286297:exon50:c.C1496G:p.T499S x3bKHL32:NM_001286298:exon51:c.C1496G:p.T499S x3bKHL32:NM_001286299:exon52:c.C1496G:p.T499S x3bKHL32:NM_001286210:exon53:c.C1496G:p.T499S x3bKHL32:NM_001286211:exon54:c.C1496G:p.T499S x3bKHL32:NM_001286212:exon55:c.C1496G:p.T499S x3bKHL32:NM_001286213:exon56:c.C1496G:p.T499S x3bKHL32:NM_001286214:exon57:c.C1496G:p.T499S x3bKHL32:NM_001286215:exon58:c.C1496G:p.T499S x3bKHL32:NM_001286216:exon59:c.C1496G:p.T499S x3bKHL32:NM_001286217:exon60:c.C1496G:p.T499S x3bKHL32:NM_001286218:exon61:c.C1496G:p.T499S x3bKHL32:NM_001286219:exon62:c.C1496G:p.T499S x3bKHL32:NM_001286220:exon63:c.C1496G:p.T499S x3bKHL32:NM_001286221:exon64:c.C1496G:p.T499S x3bKHL32:NM_001286222:exon65:c.C1496G:p.T499S x3bKHL32:NM_001286223:exon66:c.C1496G:p.T499S x3bKHL32:NM_001286224:exon67:c.C1496G:p.T499S x3bKHL32:NM_001286225:exon68:c.C1496G:p.T499S x3bKHL32:NM_001286226:exon69:c.C1496G:p.T499S x3bKHL32:NM_001286227:exon70:c.C1496G:p.T499S x3bKHL32:NM_001286228:exon71:c.C1496G:p.T499S x3bKHL32:NM_001286229:exon72:c.C1496G:p.T499S x3bKHL32:NM_001286230:exon73:c.C1496G:p.T499S x3bKHL32:NM_001286231:exon74:c.C1496G:p.T499S x3bKHL32:NM_001286232:exon75:c.C1496G:p.T499S x3bKHL32:NM_001286233:exon76:c.C1496G:p.T499S x3bKHL32:NM_001286234:exon77:c.C1496G:p.T499S x3bKHL32:NM_001286235:exon78:c.C1496G:p.T499S x3bKHL32:NM_001286236:exon79:c.C1496G:p.T499S x3bKHL32:NM_001286237:exon80:c.C1496G:p.T499S x3bKHL32:NM_001286238:exon81:c.C1496G:p.T499S x3bKHL32:NM_001286239:exon82:c.C1496G:p.T499S x3bKHL32:NM_001286240:exon83:c.C1496G:p.T499S x3bKHL32:NM_001286241:exon84:c.C1496G:p.T499S x3bKHL32:NM_001286242:exon85:c.C1496G:p.T499S x3bKHL32:NM_001286243:exon86:c.C1496G:p.T499S x3bKHL32:NM_001286244:exon87:c.C1496G:p.T499S x3bKHL32:NM_001286245:exon88:c.C1496G:p.T499S x3bKHL32:NM_001286246:exon89:c.C1496G:p.T499S x3bKHL32:NM_001286247:exon90:c.C1496G:p.T499S x3bKHL32:NM_001286248:exon91:c.C1496G:p.T499S x3bKHL32:NM_001286249:exon92:c.C1496G:p.T499S x3bKHL32:NM_001286250:exon93:c.C1496G:p.T499S x3bKHL32:NM_001286251:exon94:c.C1496G:p.T499S x3bKHL32:NM_001286252:exon95:c.C1496G:p.T499S x3bKHL32:NM_001286253:exon96:c.C1496G:p.T499S x3bKHL32:NM_001286254:exon97:c.C1496G:p.T499S x3bKHL32:NM_001286255:exon98:c.C1496G:p.T499S x3bKHL32:NM_001286256:exon99:c.C1496G:p.T499S x3bKHL32:NM_001286257:exon100:c.C1496G:p.T499S x3bKHL32:NM_001286258:exon101:c.C1496G:p.T499S x3bKHL32:NM_001286259:exon102:c.C1496G:p.T499S x3bKHL32:NM_001286260:exon103:c.C1496G:p.T499S x3bKHL32:NM_001286261:exon104:c.C1496G:p.T499S x3bKHL32:NM_001286262:exon105:c.C1496G:p.T499S x3bKHL32:NM_001286263:exon106:c.C1496G:p.T499S x3bKHL32:NM_001286264:exon107:c.C1496G:p.T499S x3bKHL32:NM_001286265:exon108:c.C1496G:p.T499S x3bKHL32:NM_001286266:exon109:c.C1496G:p.T499S x3bKHL32:NM_001286267:exon110:c.C1496G:p.T499S x3bKHL32:NM_001286268:exon111:c.C1496G:p.T499S x3bKHL32:NM_001286269:exon112:c.C1496G:p.T499S x3bKHL32:NM_001286270:exon113:c.C1496G:p.T499S x3bKHL32:NM_001286271:exon114:c.C1496G:p.T499S x3bKHL32:NM_001286272:exon115:c.C1496G:p.T499S x3bKHL32:NM_001286273:exon116:c.C1496G:p.T499S x3bKHL32:NM_001286274:exon117:c.C1496G:p.T499S x3bKHL32:NM_001286275:exon118:c.C1496G:p.T499S x3bKHL32:NM_001286276:exon119:c.C1496G:p.T499S x3bKHL32:NM_001286277:exon120:c.C1496G:p.T499S x3bKHL32:NM_001286278:exon121:c.C1496G:p.T499S x3bKHL32:NM_001286279:exon122:c.C1496G:p.T499S x3bKHL32:NM_001286280:exon123:c.C1496G:p.T499S x3bKHL32:NM_001286281:exon124:c.C1496G:p.T499S x3bKHL32:NM_001286282:exon125:c.C1496G:p.T499S x3bKHL32:NM_001286283:exon126:c.C1496G:p.T499S x3bKHL32:NM_001286284:exon127:c.C1496G:p.T499S x3bKHL32:NM_001286285:exon128:c.C1496G:p.T499S x3bKHL32:NM_001286286:exon129:c.C1496G:p.T499S x3bKHL32:NM_001286287:exon130:c.C1496G:p.T499S x3bKHL32:NM_001286288:exon131:c.C1496G:p.T499S x3bKHL32:NM_001286289:exon132:c.C1496G:p.T499S x3bKHL32:NM_001286290:exon133:c.C1496G:p.T499S x3bKHL32:NM_001286291:exon134:c.C1496G:p.T499S x3bKHL32:NM_001286292:exon135:c.C1496G:p.T499S x3bKHL32:NM_001286293:exon136:c.C1496G:p.T499S x3bKHL32:NM_001286294:exon137:c.C1496G:p.T499S x3bKHL32:NM_001286295:exon138:c.C1496G:p.T499S x3bKHL32:NM_001286296:exon139:c.C1496G:p.T499S x3bKHL32:NM_001286297:exon140:c.C1496G:p.T499S x3bKHL32:NM_001286298:exon141:c.C1496G:p.T499S x3bKHL32:NM_001286299:exon142:c.C1496G:p.T499S x3bKHL32:NM_001286300:exon143:c.C1496G:p.T499S x3bKHL32:NM_001286301:exon144:c.C1496G:p.T499S x3bKHL32:NM_001286302:exon145:c.C1496G:p.T499S x3bKHL32:NM_001286303:exon146:c.C1496G:p.T499S x3bKHL32:NM_001286304:exon147:c.C1496G:p.T499S x3bKHL32:NM_001286305:exon148:c.C1496G:p.T499S x3bKHL32:NM_001286306:exon149:c.C1496G:p.T499S x3bKHL32:NM_001286307:exon150:c.C1496G:p.T499S x3bKHL32:NM_001286308:exon151:c.C1496G:p.T499S x3bKHL32:NM_001286309:exon152:c.C1496G:p.T499S x3bKHL32:NM_001286310:exon153:c.C1496G:p.T499S x3bKHL32:NM_001286311:exon154:c.C1496G:p.T499S x3bKHL32:NM_001286312:exon155:c.C1496G:p.T499S x3bKHL32:NM_001286313:exon156:c.C1496G:p.T499S x3bKHL32:NM_001286314:exon157:c.C1496G:p.T499S x3bKHL32:NM_001286315:exon158:c.C1496G:p.T499S x3bKHL32:NM_001286316:exon159:c.C1496G:p.T499S x3bKHL32:NM_001286317:exon160:c.C1496G:p.T499S x3bKHL32:NM_001286318:exon161:c.C1496G:p.T499S x3bKHL32:NM_001286319:exon162:c.C1496G:p.T499S x3bKHL32:NM_001286320:exon163:c.C1496G:p.T499S x3bKHL32:NM_001286321:exon164:c.C1496G:p.T499S x3bKHL32:NM_001286322:exon165:c.C1496G:p.T499S x3bKHL32:NM_001286323:exon166:c.C1496G:p.T499S x3bKHL32:NM_001286324:exon167:c.C1496G:p.T499S x3bKHL32:NM_001286325:exon168:c.C1496G:p.T499S x3bKHL32:NM_001286326:exon169:c.C1496G:p.T499S x3bKHL32:NM_001286327:exon170:c.C1496G:p.T499S x3bKHL32:NM_001286328:exon171:c.C1496G:p.T499S x3bKHL32:NM_001286329:exon172:c.C1496G:p.T499S x3bKHL32:NM_001286330:exon173:c.C1496G:p.T499S x3bKHL32:NM_001286331:exon174:c.C1496G:p.T499S x3bKHL32:NM_001286332:exon175:c.C1496G:p.T499S x3bKHL32:NM_001286333:exon176:c.C1496G:p.T499S x3bKHL32:NM_001286334:exon177:c.C1496G:p.T499S x3bKHL32:NM_001286335:exon178:c.C1496G:p.T499S x3bKHL32:NM_001286336:exon179:c.C1496G:p.T499S x3bKHL32:NM_001286337:exon180:c.C1496G:p.T499S x3bKHL32:NM_001286338:exon181:c.C1496G:p.T499S x3bKHL32:NM_001286339:exon182:c.C1496G:p.T499S x3bKHL32:NM_001286340:exon183:c.C1496G:p.T499S x3bKHL32:NM_001286341:exon184:c.C1496G:p.T499S x3bKHL32:NM_001286342:exon185:c.C1496G:p.T499S x3bKHL32:NM_001286343:exon186:c.C1496G:p.T499S x3bKHL32:NM_001286344:exon187:c.C1496G:p.T499S x3bKHL32:NM_001286345:exon188:c.C1496G:p.T499S x3bKHL32:NM_001286346:exon189:c.C1496G:p.T499S x3bKHL32:NM_001286347:exon190:c.C1496G:p.T499S x3bKHL32:NM_001286348:exon191:c.C1496G:p.T499S x3bKHL32:NM_001286349:exon192:c.C1496G:p.T499S x3bKHL32:NM_001286350:exon193:c.C1496G:p.T499S x3bKHL32:NM_001286351:exon194:c.C1496G:p.T499S x3bKHL32:NM_001286352:exon195:c.C1496G:p.T499S x3bKHL32:NM_001286353:exon196:c.C1496G:p.T499S x3bKHL32:NM_001286354:exon197:c.C1496G:p.T499S x3bKHL32:NM_001286355:exon198:c.C1496G:p.T499S x3bKHL32:NM_001286356:exon199:c.C1496G:p.T499S x3bKHL32:NM_001286357:exon200:c.C1496G:p.T499S x3bKHL32:NM_001286358:exon201:c.C1496G:p.T499S x3bKHL32:NM_001286359:exon202:c.C1496G:p.T499S x3bKHL32:NM_001286360:exon203:c.C1496G:p.T499S x3bKHL32:NM_001286361:exon204:c.C1496G:p.T499S x3bKHL32:NM_001286362:exon205:c.C1496G:p.T499S x3bKHL32:NM_001286363:exon206:c.C1496G:p.T499S x3bKHL32:NM_001286364:exon207:c.C1496G:p.T499S x3bKHL32:NM_001286365:exon208:c.C1496G:p.T499S x3bKHL32:NM_001286366:exon209:c.C1496G:p.T499S x3bKHL32:NM_001286367:exon210:c.C1496G:p.T499S x3bKHL32:NM_001286368:exon211:c.C1496G:p.T499S x3bKHL32:NM_001286369:exon212:c.C1496G:p.T499S x3bKHL32:NM_001286370:exon213:c.C1496G:p.T499S x3bKHL32:NM_001286371:exon214:c.C1496G:p.T499S x3bKHL32:NM_001286372:exon215:c.C1496G:p.T499S x3bKHL32:NM_001286373:exon216:c.C1496G:p.T499S x3bKHL32:NM_001286374:exon217:c.C1496G:p.T499S x3bKHL32:NM_001286375:exon218:c.C1496G:p.T499S x3bKHL32:NM_001286376:exon219:c.C1496G:p.T499S x3bKHL32:NM_001286377:exon220:c.C1496G:p.T499S x3bKHL32:NM_001286378:exon221:c.C1496G:p.T499S x3bKHL32:NM_001286379:exon222:c.C1496G:p.T499S x3bKHL32:NM_001286380:exon223:c.C1496G:p.T499S x3bKHL32:NM_001286381:exon224:c.C1496G:p.T499S x3bKHL32:NM_001286382:exon225:c.C1496G:p.T499S x3bKHL32:NM_001286383:exon226:c.C1496G:p.T499S x3bKHL32:NM_001286384:exon227:c.C1496G:p.T499S x3bKHL32:NM_001286385:exon228:c.C1496G:p.T499S x3bKHL32:NM_001286386:exon229:c.C1496G:p.T499S x3bKHL32:NM_001286387:exon230:c.C1496G:p.T499S x3bKHL32:NM_001286388:exon231:c.C1496G:p.T499S x3bKHL32:NM_001286389:exon

31872251:CA	MetaPan.NET-5	HEATR5A	HEATR5A:NM_015473:exon28:c.G4364T:p.R1455I
2:23633259:G:C	MetaPan.NET-2	KCNJ13	KCNJ13:NM_001172417:exon3:c.C485T:p.T162M>x3bKCNJ13:NM_002242:exon3:c.C725T:p.T242M
14:9420789:CA	MetaPan.NET-5	ASB2	ASB2:NM_016150:exon2:c.G208T:p.R70K>x3bASB2:NM_00120249:exon4:c.G352T:p.E118X
3:195508476:G:C	MetaPan.NET-4	MUC4	MUC4:NM_018406:exon2:c.C9975G:p.H3325Q
3:194147849:CA:C	MetaPan.NET-5	ATP13A3	ATP13A3:NM_0024524:exon2:c.3079delT:p.W1027fs
3:195512690:G:C	MetaPan.NET-4	MUC4	MUC4:NM_018406:exon2:c.C5761L:p.L1921V
X:155169442:CA	MetaPan.NET-5	VAMP7	VAMP7:NM_001185183:exon6:c.C511A:p.H71N
20:33734701:T:TCGT	MetaPan.NET-14	EDEM2	EDEM2:NM_018217:exon2:c.I42_144del:p.48_48del
18:11725923:G:T	MetaPan.NET-8	GNAL	GNAL:NM_182978:exon2:c.G448T:p.I150X>x3bGNAL:NM_001142339:exon3:c.G217T:p.E73X>x3bGNAL:NM_001216443:exon3:c.G217T:p.E73X
17:47895308:CT	MetaPan.NET-13	KAT7	KAT7:NM_001199158:exon6:c.C583T:p.R195C>x3bKAT7:NM_001199157:exon7:c.C673T:p.R225C>x3bKAT7:NM_001199157:exon7:c.C760T:p.R254C>x3bKAT7:NM_001199157
16:68324373:T:A	MetaPan.NET-16	SLC7A6	SLC7A6:NM_003983:exon5:c.T724A:p.S242T>x3bSLC7A6:NM_001076785:exon6:c.T724A:p.S242T
19:4512315:C:T	MetaPan.NET-2	PLIN4	PLIN4:NM_01080400:exon3:c.G615A:p.G595
3:195506363:CT	MetaPan.NET-14	MUC4	MUC4:NM_018406:exon2:c.D1208A:p.A4030T
21:46924434:A:C	MetaPan.NET-2	COT18A1	.
6:33287156:CA	MetaPan.NET-8	DAXX	.
3:126740965:G:A	MetaPan.NET-4	PLXNA1	PLXNA1:NM_032242:exon21:c.G4076A:p.G1359E
17:74160838:CG	MetaPan.NET-17	RNF157	RNF157:NM_0052916:exon8:c.G711C:p.Q237H
1:3416277:C	MetaPan.NET-14	MEGF6	MEGF6:NM_001409:exon23:c.G2804T:p.Q947F
12:11373080:T:C	MetaPan.NET-20	TPCN1	TPCN1:NM_001301214:exon25:c.C1978T:p.R660W>x3bTPCN1:NM_017901:exon26:c.C2182T:p.R728W>x3bTPCN1:NM_001143819:exon27:c.C2398T:p.R800W
15:54080841:G:A	MetaPan.NET-5	ZNF331	ZNF331:NM_001253801:exon5:c.G1027A:p.V343I>x3bZNF331:NM_001079906:exon6:c.G1027A:p.V343I>x3bZNF331:NM_001079907:exon6:c.G1027A:p.V343I>x3bZNF331:NM_001079907
3:195509108:T:A	MetaPan.NET-4	MUC4	MUC4:NM_018406:exon2:c.A9343T:p.T3115S
16:74183578:G:A	MetaPan.NET-18	ZNF23	ZNF23:NM_001304494:exon3:c.T176C:p.V57C>x3bZNF23:NM_001304492:exon5:c.T350C:p.V117A>x3bZNF23:NM_001304492
12:22063235:CT	MetaPan.NET-1	ABCC9	ABCC9:NM_005691:exon8:c.T1176A:p.Y392K>x3bABCC9:NM_020297:exon8:c.T1176A:p.Y392K
5:140428526:CT	MetaPan.NET-5	PCDH8	PCDH8:NM_018937:exon1:c.C2329T:p.Q777X
6:32609297:GT	MetaPan.NET-16	HLA-DQA1	HLA-DQA1:NM_002122:exon2:c.T293G:p.I98S
11:64572060:G:A	MetaPan.NET-3	MEN1	MEN1:NM_000244:exon10:c.C1594T:p.R522X>x3bMEN1:NM_130799:exon10:c.C1597T:p.R527X>x3bMEN1:NM_130800:exon10:c.C1594T:p.R532X>x3bMEN1:NM_130801:ex
22:2985602:AC	MetaPan.NET-13	NEFH	NEFH:NM_021076:exon4:c.A1973C:p.F658A
X:150349560:CT	MetaPan.NET-4	GPR50	GPR50:NM_002424:exon2:c.K1505T:p.T502I
19:25511534:TA	MetaPan.NET-5	MUC4	MUC4:NM_018406:exon2:c.G6917T:p.H2306L
13:25479645:G:C	MetaPan.NET-17	CENPJ	CENPJ:NM_018451:exon7:c.C2531G:p.P84R
11:64577442:T:TAGCAGGGTTGA:T	MetaPan.NET-5	MEN1	MEN1:NM_000244:exon2:c.149_159del:p.V50fs>x3bMEN1:NM_130799:exon2:c.149_159del:p.V50fs>x3bMEN1:NM_130800:exon2:c.149_159del:p.V50fs>x3bMEN1:NM_130801:ex
1:17086088:G:C	MetaPan.NET-6	MST1L	MST1L:NM_001271733:exon7:c.G1027A:p.A270G
12:10283410:CA	MetaPan.NET-17	GALNT9	GALNT9:NM_001221636:exon5:c.G577T:p.G293C
6:109282798:G:A	MetaPan.NET-5	ARM2C	ARM2C:NM_021076:exon4:c.A1973C:p.F658A
2:20819111:AG	MetaPan.NET-12	SMARCA2	SMARCA2:NM_001289396:exon15:c.A2264G:p.K755R>x3bSMARCA2:NM_003070:exon15:c.A2264G:p.K755R>x3bSMARCA2:NM_003070
3:58090867:TG:T	MetaPan.NET-6	FLNB	FLNB:NM_001164317:exon11:c.1672delG:p.G558fs>x3bFLNB:NM_001164318:exon11:c.1672delG:p.G558fs>x3bFLNB:NM_001164318
10:55996618:CT	MetaPan.NET-17	PCDH15	PCDH15:NM_001142767:exon8:c.C839A:p.S280X>x3bPCDH15:NM_001142768:exon8:c.C884A:p.S295X>x3bPCDH15:NM_001142773:exon8:c.C884A:p.S295X>x3bPCDH15:NM_001142773
17:47395806:T:A	MetaPan.NET-18	UBE2O	UBE2O:NM_022066:exon9:c.A1352T:p.E451V
3:195515052:G:C	MetaPan.NET-12	MUC4	MUC4:NM_018406:exon2:c.C3399G:p.H113Q
5:140789433:GT	MetaPan.NET-5	PCDHGB6	PCDHGB6:NM_018926:exon1:c.G1892C:p.R555L>x3bPCDHGB6:NM_032100:exon1:c.G1664T:p.R555L
3:195508668:G:C	MetaPan.NET-1	MUC4	MUC4:NM_018406:exon2:c.K9783C:p.D3261E
19:11130283:G:T	MetaPan.NET-5	SMARCA4	SMARCA4:NM_001128845:exon17:c.G2522T:p.R841I>x3bSMARCA4:NM_001128846:exon17:c.G2522T:p.R841I>x3bSMARCA4:NM_001128847:exon17:c.G2522T:p.R841I>x3bSMARCA4:NM_001128847
7:10505510:AT	MetaPan.NET-13	MUC3A	MUC3A:NM_005960:exon2:c.A10917T:p.E364V
18:31401310:G:A	MetaPan.NET-18	CHRD	CHRD:NM_001304047:exon16:c.G558R:p.G558R>x3bCHRD:NM_001304474:exon16:c.G853A:p.G285R>x3bCHRD:NM_001304474
20:36488419:GT	MetaPan.NET-5	CTNNBL1	CTNNBL1:NM_030877:exon14:c.G1511T:p.C504F>x3bCTNNBL1:NM_01281495:exon15:c.G1430T:p.C477F
10:7614318:CA	MetaPan.NET-2	ITIH5	ITIH5:NM_001001851:exon12:c.G2076T:p.M692I
2:214727222:CT	MetaPan.NET-11	SPAG16	SPAG16:NM_024532:exon11:c.C1084T:p.P362S
10:3592808:CA	MetaPan.NET-17	F2D8	F2D8:NM_031866:exon11:c.G1552T:p.D518Y
21:11058316:G:T	MetaPan.NET-5	BAGE2>x3bBAGE3	BAGE3:NM_182481:exon3:c.C124A:p.H42N>x3bBAGE2:NM_182482:exon3:c.C124A:p.H42N
19:40541423:CTCA:CC	MetaPan.NET-15	ZNF780B	ZNF780B:NM_001005851:exon5:c.I339_1342del:p.C447fs
4:6925490:G:A	MetaPan.NET-16	TBC1D14	TBC1D14:NM_001113361:exon2:c.G374A:p.R125H>x3bTBC1D14:NM_020773:exon2:c.G374A:p.R125H
6:86328541:AT	MetaPan.NET-4	SYNCRIP	SYNCRIP:NM_001159673:exon9:c.980dup0:NM_0327fs>x3bSYNCRIP:NM_001159675:exon9:c.1169dupA:p.N390fs>x3bSYNCRIP:NM_001159676:exon9:c.1274dupA:p.N425fs>x3bSYNCRIP:NM_001159676
11:30033412:CG	MetaPan.NET-17	KCNA4	KCNA4:NM_002233:exon2:c.G814C:p.D272H
12:152515622:G:A	MetaPan.NET-3	NEB	NEB:NM_001164507:exon7:c.G6302T:p.P2011L>x3bNEB:NM_001164508:exon47:c.C6032T:p.P2011L>x3bNEB:NM_001271208:exon47:c.C6032T:p.P2011L>x3bNEB:NM_001271208
1:1585081:CT	MetaPan.NET-17	P2RY8	P2RY8:NM_178129:exon2:c.G371A:p.G214E
2:238529021:CA	MetaPan.NET-5	PLA2G6	.
1:234593420:CT	MetaPan.NET-2	TARBP1	TARBP1:NM_005646:exon9:c.G175A:p.W572X
11:85375244:T:C	MetaPan.NET-8	CREBF2	CREBF2:NM_001039618:exon1:c.A676G:p.K226E
6:168376927:G:C	MetaPan.NET-13	HGC6.3	HGC6.3:NM_001129895:exon1:c.C406G:p.P136A
13:37781808:G:C	MetaPan.NET-4	MYCP2	MYCP2:NM_015057:exon16:c.C2385G:p.T795M
13:10198845:CA	MetaPan.NET-12	SPDY6	SPDY6:NM_001146210:exon6:c.G1028T:p.R343L
12:203875:CG	MetaPan.NET-3	FGD2	FGD2:NM_17358:exon5:c.G677A:p.R226H
1:172404474:GA	MetaPan.NET-16	ARAP1	ARAP1:NM_001135190:exon26:c.C2932T:p.R978C>x3bARAP1:NM_015242:exon27:c.C3115T:p.R1039C>x3bARAP1:NM_001040118:exon29:c.C3850T:p.R1284C
1:20577889:CTTCCTTTGTG:C	MetaPan.NET-17	ATRX	ATRX:NM_132870:exon30:c.6664_6675del:p.2222_2225del>x3bATRX:NM_000489:exon31:c.6778_6789del:p.2260_2263del
2:212295786:CA	MetaPan.NET-2	ERBB4	ERBB4:NM_001042599:exon21:c.G2527T:p.D843Y>x3bERBB4:NM_005235:exon21:c.G2527T:p.D843Y
1:17677889:CTTCCTTTGTG:C	MetaPan.NET-17	ITIH5	ITIH5:NM_001001851:exon12:c.G2076T:p.M692I
1:2112295786:CA	MetaPan.NET-20	VWA5B2	VWA5B2:NM_138345:exon4:c.C668G:p.T223S
1:164111357:CA	MetaPan.NET-3	CCDC88B	CCDC88B:NM_032251:exon13:c.C1426A:p.Q476K
17:77808:NM_00128845:CT	MetaPan.NET-11	CDCC40	CDCC40:NM_001243342:exon15:c.C2561T:p.S854L>x3bCCDC40:NM_017950:exon15:c.C2561T:p.S854L
1:119434243:CG	MetaPan.NET-12	ZNF440	ZNF440:NM_0152357:exon4:c.C1252G:p.H418D
16:1550157:CA	MetaPan.NET-5	TELO2	TELO2:NM_0161111:exon7:c.C994A:p.L323M
1:45976870:G:A	MetaPan.NET-5	MUTYH	MUTYH:NM_001048171:exon14:c.C1418T:p.S473F>x3bMUTYH:NM_001048172:exon14:c.C1379T:p.S460F>x3bMUTYH:NM_001048173:exon14:c.C1376T:p.S459F>x3bMUTYH:NM_001048173
12:53682047:G:A	MetaPan.NET-5	ESPL1	ESPL1:NM_012291:exon9:c.G4468A:p.E1940K
2:26461997:CA	MetaPan.NET-16	HADHA	HADHA:NM_000182:exon2:c.G80A:p.R27H
3:4768820:CA	MetaPan.NET-5	TPR1	TPR1:NM_001168272:exon4:c.C5138A:p.P1713Q
12:122426114:G:T	MetaPan.NET-17	SETD1B	SETD1B:NM_015048:exon4:c.G545T:p.G182V
16:52479493:G:A	MetaPan.NET-5	TOX3	TOX3:NM_001084030:exon3:c.C3117T:p.P104L>x3bTOX3:NM_001146188:exon4:c.C296T:p.P99L
15:48773869:CT	MetaPan.NET-5	FBN1	FBN1:NM_000138:exon32:c.G3947A:p.G1316E
12:309012506:CA	MetaPan.NET-12	CAPRIN2	CAPRIN2:NM_01002259:exon1:c.G374T:p.R125V>x3bCAPRIN2:NM_001206856:exon1:c.G374T:p.R125V>x3bCAPRIN2:NM_023925:exon1:c.G374T:p.G125V>x3bCAPRIN2:NM_023925
6:152680550:G:A	MetaPan.NET-18	SYNE1	SYNE1:NM_003071:exon65:c.C10347T:p.T3455X>x3bSYNE1:NM_182961:exon65:c.C10347T:p.T3448I
16:68276908:CA	MetaPan.NET-20	ESRP2	ESRP2:NM_024939:exon3:c.G4307T:p.A144S
18:19348598:CT	MetaPan.NET-1	MIB1	MIB1:NM_002774:exon3:c.C416T:p.S139F
1:173604925:G:A	MetaPan.NET-2	LOC730159	LOC730159:NM_001195190:exon1:c.G265A:p.V89I
12:46244018:AT	MetaPan.NET-9	ARD12	ARD12:NM_152641:exon15:c.A2112T:p.Q704H
3:77576567:T:A	MetaPan.NET-14	ROBO2	.
6:78538672:CA:G	MetaPan.NET-1	ME14	ME14:NM_001282136:exon3:c.T794_795del:p.Q265fs
12:40882545:CT	MetaPan.NET-15	MUC19	UNKNOWN
6:109771594:GA	MetaPan.NET-3	MICAL1	MICAL1:NM_001286613:exon8:c.C1157T:p.T386M>x3bMICAL1:NM_022765:exon8:c.C1100T:p.T367M
12:9312546:GT	MetaPan.NET-16	P2P	P2P:NM_002864:exon25:c.3124delC:p.C1042fs
13:54357325:AT	MetaPan.NET-17	CREM	CREM:NM_001881:exon2:c.A267T:p.Q9L>x3bCREM:NM_183011:exon2:c.A74T:p.Q25L>x3bCREM:NM_183012:exon2:c.A74T:p.Q25L>x3bCREM:NM_183060:exon2:c.A267T:p.Q25L>x3bCREM:NM_183060
12:50428334:CA	MetaPan.NET-16	SMARCD1	SMARCD1:NM_003076:exon6:c.G685T:p.Q229X>x3bSMARCD1:NM_139071:exon6:c.G685T:p.Q229X
1:469157674:CA	MetaPan.NET-5	CCDC8	CCDC8:NM_032040:exon1:c.G3047T:p.A102S
2:221879121:AT	MetaPan.NET-5	MICAL3	MICAL3:NM_00122731:exon8:c.T1213A:p.W405R>x3bMICAL3:NM_001136004:exon8:c.T1213A:p.W405R>x3bMICAL3:NM_015241:exon9:c.T1213A:p.W405R
4:79205585:G:C	MetaPan.NET-13	FRAS1	.
3:121200635:CT	MetaPan.NET-6	POLQ	POLQ:NM_199420:exon19:c.G5959A:p.D1999N
4:79455668:CT	MetaPan.NET-20	FRAS1	FRAS1:NM_025074:exon71:c.C10991T:p.T6746I
6:160211646:GTT:G	MetaPan.NET-1	MIRPL18	MIRPL18:NM_014161:exon1:c.28_29del:p.L10fs
16:58953731:TA	MetaPan.NET-8	IRF8	IRF8:NM_002163:exon8:c.T1005A:p.Y335X
11:92087299:G:A	MetaPan.NET-14	FAT3	FAT3:NM_001008781:exon1:c.G2021T:p.G674V
3:121527787:CT	MetaPan.NET-6	IQC8B1	IQC8B1:NM_001203570:exon6:c.G4636A:p.G1555>x3bIQC8B1:NM_001023571:exon6:c.G4636A:p.G1555
4:71700588:CA	MetaPan.NET-3	AADAT	AADAT:NM_016228:exon2:p.K69X>x3bAADAT:NM_001286682:exon3:c.A2107T:p.K73X>x3bAADAT:NM_001286682:exon3:c.A205T:p.K69X>x3bAADAT:NM_182662:exon3:c.A205T:p.K69X>x3bAADAT:NM_182662
7:107108637:AG	MetaPan.NET-16	HCKD1	HCKD1:NM_025130:exon15:c.A2138C:p.D713G
6:112671532:G:A	MetaPan.NET-17	RPLP4B	RPLP4B:NM_001013734:exon3:c.G622A:p.G208R
8:24157580:CA	MetaPan.NET-14	ADAM28	ADAM28:NM_01034531:exon2:c.C140A:p.P47Q>x3bADAM28:NM_014265:exon2:c.C140A:p.P47Q>x3bADAM28:NM_021777:exon2:c.C140A:p.P47Q
12:26648392:CT	MetaPan.NET-5	POLD1P2	UNKNOWN
10:47853310:AG:A	MetaPan.NET-10	PPBP	PPBP:NM_002704:exon2:c.207delC:p.T69fs
1:96176738:CT	MetaPan.NET-6	DIAPH2	DIAPH2:NM_006729:exon6:c.G646T:p.L126F>x3bDIAPH2:NM_007309:exon6:c.G646T:p.L126F
10:90767463:G:C	MetaPan.NET-14	FAS	FAS:NM_000433:exon3:c.G203C:p.R68T>x3bFAS:NM_152871:exon3:c.G203C:p.R68T>x3bFAS:NM_152872:exon3:c.G203C:p.R68T
1:190423810:AT	MetaPan.NET-15	ELMIN1	ELMIN1:NM_007046:exon4:c.G1781A:p.R594H
6:136593131:A:C	MetaPan.NET-13	BRNP3	BRNP3:NM_199051:exon2:c.T211A:p.P7F1
1:X1076292:CT	MetaPan.NET-17	CLCN4	CLCN4:NM_001256944:exon7:c.C769T:p.R257C>x3bCLCN4:NM_001830:exon9:c.C1051T:p.R351C
2:508470634:CG	MetaPan.NET-11	SYCP2	SYCP2:NM_014258:exon9:c.G1523C:p.R508T
1:940310618:CA	MetaPan.NET-12	ENTPD8	ENTPD8:NM_001033113:exon7:c.G691T:p.R231C>x3bENTPD8:NM_198585:exon6:c.G691T:p.R231C
1:124507014:CA:CTGAT	MetaPan.NET-1	TBRG1	TBRG1:NM_032811:exon7:c.T91_91insTGAT:p.L04fs
12:13715788:G:A	MetaPan.NET-8	GRIN2B	GRIN2B:NM_000834:exon3:c.C4384T:p.P1462S
6:854466562:G:C	MetaPan.NET-9	TBX18	TBX18:NM_001080508:exon8:c.C1575G:p.S5525

This document is a draft version of the ANUSCRIPT. It contains numerous errors, omissions, and incomplete sections. The content is as follows:

The document is a large block of text representing a manuscript. It includes several tables and figures, but they are mostly illegible due to the high level of noise and corruption. The text is primarily in black font on a white background, with some sections appearing in red or blue. The overall quality is very poor, making it difficult to extract specific information.

Supplementary Table 2. Pathologic findings and immunohistochemical/FISH status of 347 pancreatic neuroendocrine tumors.

Patient	Tumor size (cm)	Histologic grade	ALT status	ATRX expression	DAXX expression	H3K36me3 expression	ARID1A expression	CDKN2A /CEP9 ratio
1	0.6	G1	Negative	Preserved	Preserved	Preserved	Preserved	0.99 (Wild type)
2	0.6	G2	Negative	Preserved	Preserved	Preserved	Preserved	1.18 (Wild type)
3	0.6	G1	Negative	Preserved	Preserved	Preserved	Preserved	0.96 (Wild type)
4	0.6	G1	Negative	Preserved	Preserved	Preserved	Preserved	1.05 (Wild type)
5	0.6	G1	Negative	Preserved	Preserved	Preserved	Preserved	1.06 (Wild type)
6	0.7	G1	Negative	Preserved	Preserved	Preserved	Preserved	1.03 (Wild type)
7	0.7	G1	Negative	Preserved	Preserved	Preserved	Preserved	0.97 (Wild type)
8	0.7	G1	Negative	Preserved	Preserved	Preserved	Preserved	1.00 (Wild type)
9	0.7	G1	Negative	Preserved	Preserved	Preserved	Preserved	0.96 (Wild type)
10	0.7	G1	Negative	Preserved	Preserved	Preserved	Preserved	1.00 (Wild type)
11	0.8	G1	Negative	Preserved	Preserved	Preserved	Preserved	0.96 (Wild type)
12	0.8	G1	Negative	Preserved	Preserved	Preserved	Preserved	1.02 (Wild type)
13	0.8	G1	Negative	Preserved	Preserved	Preserved	Preserved	1.00 (Wild type)
14	0.8	G1	Negative	Preserved	Preserved	Preserved	Preserved	1.12 (Wild type)
15	0.8	G1	Negative	Preserved	Preserved	Preserved	Preserved	1.00 (Wild type)
16	0.9	G1	Negative	Preserved	Preserved	Preserved	Preserved	1.00 (Wild type)
17	0.9	G1	Negative	Preserved	Preserved	Preserved	Preserved	1.02 (Wild type)
18	0.9	G1	Negative	Preserved	Preserved	Preserved	Preserved	1.00 (Wild type)
19	0.9	G1	Negative	Preserved	Preserved	Preserved	Preserved	1.13 (Wild type)
20	0.9	G1	Negative	Preserved	Preserved	Preserved	Preserved	1.02 (Wild type)
21	1.0	G1	Positive	Loss	Preserved	Preserved	Preserved	1.11 (Wild type)
22	1.0	G1	Negative	Preserved	Preserved	Preserved	Preserved	1.02 (Wild type)
23	1.0	G1	Negative	Preserved	Preserved	Preserved	Preserved	1.00 (Wild type)
24	1.0	G1	Negative	Preserved	Preserved	Preserved	Preserved	0.97 (Wild type)
25	1.0	G2	Negative	Preserved	Preserved	Preserved	Preserved	1.01 (Wild type)
26	1.0	G1	Negative	Preserved	Preserved	Preserved	Preserved	0.89 (Wild type)
27	1.0	G2	Negative	Preserved	Preserved	Preserved	Preserved	1.02 (Wild type)
28	1.0	G2	Negative	Preserved	Preserved	Preserved	Preserved	1.01 (Wild type)
29	1.0	G1	Negative	Preserved	Preserved	Preserved	Preserved	1.00 (Wild type)

30	1.0	G1	Negative	Preserved	Preserved	Preserved	Preserved	1.02 (Wild type)
31	1.0	G2	Negative	Preserved	Preserved	Preserved	Preserved	1.00 (Wild type)
32	1.0	G1	Negative	Preserved	Preserved	Preserved	Preserved	0.99 (Wild type)
33	1.0	G1	Negative	Preserved	Preserved	Preserved	Preserved	0.99 (Wild type)
34	1.0	G1	Negative	Preserved	Preserved	Preserved	Preserved	0.96 (Wild type)
35	1.0	G1	Negative	Preserved	Preserved	Preserved	Preserved	1.00 (Wild type)
36	1.1	G1	Negative	Preserved	Preserved	Preserved	Preserved	0.98 (Wild type)
37	1.1	G2	Negative	Preserved	Preserved	Preserved	Preserved	1.02 (Wild type)
38	1.1	G1	Negative	Preserved	Preserved	Preserved	Preserved	0.99 (Wild type)
39	1.1	G2	Negative	Preserved	Preserved	Preserved	Preserved	0.98 (Wild type)
40	1.1	G1	Negative	Preserved	Preserved	Preserved	Preserved	1.00 (Wild type)
41	1.1	G1	Negative	Preserved	Preserved	Preserved	Preserved	1.01 (Wild type)
42	1.2	G2	Positive	Loss	Preserved	Loss	Preserved	1.00 (Wild type)
43	1.2	G1	Negative	Preserved	Preserved	Preserved	Preserved	1.00 (Wild type)
44	1.2	G2	Negative	Preserved	Preserved	Preserved	Preserved	1.03 (Wild type)
45	1.2	G1	Negative	Preserved	Preserved	Preserved	Preserved	0.93 (Wild type)
46	1.2	G1	Negative	Preserved	Preserved	Preserved	Preserved	1.05 (Wild type)
47	1.2	G1	Negative	Preserved	Preserved	Preserved	Preserved	0.91 (Wild type)
48	1.2	G2	Negative	Preserved	Preserved	Preserved	Preserved	0.95 (Wild type)
49	1.3	G1	Negative	Preserved	Preserved	Loss	Preserved	1.07 (Wild type)
50	1.3	G1	Negative	Preserved	Preserved	Preserved	Preserved	1.11 (Wild type)
51	1.3	G1	Negative	Preserved	Preserved	Preserved	Preserved	0.96 (Wild type)
52	1.3	G2	Negative	Preserved	Preserved	Preserved	Preserved	1.01 (Wild type)
53	1.3	G2	Negative	Preserved	Preserved	Preserved	Preserved	1.01 (Wild type)
54	1.3	G1	Negative	Preserved	Preserved	Preserved	Preserved	1.04 (Wild type)
55	1.3	G1	Negative	Preserved	Preserved	Preserved	Preserved	1.06 (Wild type)
56	1.3	G1	Negative	Preserved	Preserved	Preserved	Preserved	0.98 (Wild type)
57	1.3	G1	Negative	Preserved	Preserved	Preserved	Preserved	1.02 (Wild type)
58	1.3	G1	Negative	Preserved	Preserved	Preserved	Preserved	0.99 (Wild type)
59	1.3	G1	Negative	Preserved	Preserved	Preserved	Preserved	1.06 (Wild type)
60	1.4	G1	Negative	Preserved	Preserved	Preserved	Preserved	0.96 (Wild type)
61	1.4	G2	Negative	Preserved	Preserved	Preserved	Preserved	0.99 (Wild type)
62	1.4	G2	Negative	Preserved	Preserved	Preserved	Preserved	0.92 (Wild type)

63	1.4	G2	Negative	Preserved	Preserved	Preserved	Preserved	1.00 (Wild type)
64	1.4	G1	Negative	Preserved	Preserved	Preserved	Preserved	0.98 (Wild type)
65	1.4	G1	Negative	Preserved	Preserved	Preserved	Preserved	1.02 (Wild type)
66	1.4	G1	Negative	Preserved	Preserved	Preserved	Preserved	0.99 (Wild type)
67	1.5	G2	Negative	Preserved	Preserved	Loss	Preserved	1.00 (Wild type)
68	1.5	G1	Positive	Preserved	Loss	Preserved	Preserved	0.95 (Wild type)
69	1.5	G1	Negative	Preserved	Preserved	Preserved	Preserved	0.88 (Wild type)
70	1.5	G1	Negative	Preserved	Preserved	Preserved	Preserved	1.00 (Wild type)
71	1.5	G1	Negative	Preserved	Preserved	Preserved	Preserved	0.99 (Wild type)
72	1.5	G1	Negative	Preserved	Preserved	Preserved	Preserved	0.98 (Wild type)
73	1.5	G1	Negative	Preserved	Preserved	Preserved	Preserved	1.02 (Wild type)
74	1.5	G1	Negative	Preserved	Preserved	Preserved	Preserved	1.05 (Wild type)
75	1.5	G1	Negative	Preserved	Preserved	Preserved	Preserved	1.06 (Wild type)
76	1.5	G1	Negative	Preserved	Preserved	Preserved	Preserved	1.04 (Wild type)
77	1.5	G1	Negative	Preserved	Preserved	Preserved	Preserved	0.97 (Wild type)
78	1.5	G1	Negative	Preserved	Preserved	Preserved	Preserved	1.03 (Wild type)
79	1.5	G1	Negative	Preserved	Preserved	Preserved	Preserved	1.07 (Wild type)
80	1.5	G2	Negative	Preserved	Preserved	Preserved	Preserved	1.22 (Wild type)
81	1.5	G2	Negative	Preserved	Preserved	Preserved	Preserved	1.01 (Wild type)
82	1.5	G2	Negative	Preserved	Preserved	Preserved	Preserved	1.06 (Wild type)
83	1.5	G1	Negative	Preserved	Preserved	Preserved	Preserved	0.99 (Wild type)
84	1.5	G2	Negative	Preserved	Preserved	Preserved	Preserved	0.96 (Wild type)
85	1.5	G1	Negative	Preserved	Preserved	Preserved	Preserved	1.03 (Wild type)
86	1.5	G1	Negative	Preserved	Preserved	Preserved	Preserved	0.99 (Wild type)
87	1.5	G1	Negative	Preserved	Preserved	Preserved	Preserved	1.05 (Wild type)
88	1.5	G1	Negative	Preserved	Preserved	Preserved	Preserved	0.99 (Wild type)
89	1.5	G1	Negative	Preserved	Preserved	Preserved	Preserved	0.98 (Wild type)
90	1.5	G1	Negative	Preserved	Preserved	Preserved	Preserved	0.95 (Wild type)
91	1.5	G1	Negative	Preserved	Preserved	Preserved	Preserved	1.19 (Wild type)
92	1.5	G1	Negative	Preserved	Preserved	Preserved	Preserved	1.04 (Wild type)
93	1.5	G1	Negative	Preserved	Preserved	Preserved	Preserved	0.99 (Wild type)
94	1.5	G1	Negative	Preserved	Preserved	Preserved	Preserved	0.98 (Wild type)
95	1.6	G1	Negative	Preserved	Preserved	Preserved	Preserved	1.08 (Wild type)

96	1.6	G1	Negative	Preserved	Preserved	Preserved	Preserved	1.23 (Wild type)
97	1.6	G2	Negative	Preserved	Preserved	Preserved	Preserved	1.00 (Wild type)
98	1.6	G1	Negative	Preserved	Preserved	Preserved	Preserved	1.10 (Wild type)
99	1.7	G2	Positive	Preserved	Loss	Preserved	Loss	1.07 (Wild type)
100	1.7	G1	Negative	Preserved	Preserved	Preserved	Preserved	1.16 (Wild type)
101	1.7	G1	Negative	Preserved	Preserved	Preserved	Preserved	1.00 (Wild type)
102	1.7	G2	Negative	Preserved	Preserved	Preserved	Preserved	1.05 (Wild type)
103	1.7	G1	Negative	Preserved	Preserved	Preserved	Preserved	1.03 (Wild type)
104	1.7	G1	Negative	Preserved	Preserved	Preserved	Preserved	0.98 (Wild type)
105	1.7	G1	Negative	Preserved	Preserved	Preserved	Preserved	0.85 (Wild type)
106	1.8	G2	Positive	Preserved	Preserved	Preserved	Preserved	0.95 (Wild type)
107	1.8	G1	Negative	Preserved	Preserved	Preserved	Preserved	1.04 (Wild type)
108	1.8	G1	Negative	Preserved	Preserved	Preserved	Preserved	1.00 (Wild type)
109	1.8	G2	Negative	Preserved	Preserved	Preserved	Preserved	1.08 (Wild type)
110	1.8	G1	Negative	Preserved	Preserved	Preserved	Preserved	0.99 (Wild type)
111	1.8	G1	Negative	Preserved	Preserved	Preserved	Preserved	1.04 (Wild type)
112	1.8	G1	Negative	Preserved	Preserved	Preserved	Preserved	1.23 (Wild type)
113	1.9	G1	Negative	Preserved	Preserved	Preserved	Preserved	0.96 (Wild type)
114	2.0	G2	Positive	Loss	Preserved	Preserved	Preserved	0.46 (Deletion)
115	2.0	G2	Positive	Loss	Loss	Preserved	Preserved	0.65 (Deletion)
116	2.0	G2	Negative	Preserved	Preserved	Loss	Preserved	1.01 (Wild type)
117	2.0	G2	Positive	Preserved	Loss	Preserved	Preserved	0.98 (Wild type)
118	2.0	G1	Positive	Loss	Loss	Preserved	Preserved	1.04 (Wild type)
119	2.0	G1	Negative	Preserved	Preserved	Preserved	Preserved	1.04 (Wild type)
120	2.0	G1	Negative	Preserved	Preserved	Preserved	Preserved	1.00 (Wild type)
121	2.0	G1	Negative	Preserved	Preserved	Preserved	Preserved	1.10 (Wild type)
122	2.0	G1	Negative	Preserved	Preserved	Preserved	Preserved	1.00 (Wild type)
123	2.0	G1	Negative	Preserved	Preserved	Preserved	Preserved	1.15 (Wild type)
124	2.0	G2	Negative	Preserved	Preserved	Preserved	Preserved	1.03 (Wild type)
125	2.0	G1	Negative	Preserved	Preserved	Preserved	Preserved	1.04 (Wild type)
126	2.0	G1	Negative	Preserved	Preserved	Preserved	Preserved	1.01 (Wild type)
127	2.0	G2	Negative	Preserved	Preserved	Preserved	Preserved	1.01 (Wild type)
128	2.0	G2	Negative	Preserved	Preserved	Preserved	Preserved	0.96 (Wild type)

129	2.0	G1	Negative	Preserved	Preserved	Preserved	Preserved	1.07 (Wild type)
130	2.0	G1	Negative	Preserved	Preserved	Preserved	Preserved	1.01 (Wild type)
131	2.1	G1	Negative	Preserved	Preserved	Preserved	Preserved	0.96 (Wild type)
132	2.1	G1	Negative	Preserved	Preserved	Preserved	Preserved	0.97 (Wild type)
133	2.1	G2	Negative	Preserved	Preserved	Preserved	Preserved	0.94 (Wild type)
134	2.1	G1	Negative	Preserved	Preserved	Preserved	Preserved	1.03 (Wild type)
135	2.1	G2	Negative	Preserved	Preserved	Preserved	Preserved	1.05 (Wild type)
136	2.1	G1	Negative	Preserved	Preserved	Preserved	Preserved	0.98 (Wild type)
137	2.1	G2	Negative	Preserved	Preserved	Preserved	Preserved	1.11 (Wild type)
138	2.2	G1	Positive	Preserved	Loss	Preserved	Preserved	1.02 (Wild type)
139	2.2	G1	Negative	Preserved	Preserved	Preserved	Preserved	1.00 (Wild type)
140	2.2	G1	Negative	Preserved	Preserved	Preserved	Preserved	1.17 (Wild type)
141	2.2	G1	Negative	Preserved	Preserved	Preserved	Preserved	0.96 (Wild type)
142	2.2	G1	Negative	Preserved	Preserved	Preserved	Preserved	0.94 (Wild type)
143	2.2	G1	Negative	Preserved	Preserved	Preserved	Preserved	1.02 (Wild type)
144	2.2	G1	Negative	Preserved	Preserved	Preserved	Preserved	1.01 (Wild type)
145	2.2	G1	Negative	Preserved	Preserved	Preserved	Preserved	1.00 (Wild type)
146	2.3	G1	Negative	Preserved	Preserved	Preserved	Preserved	0.98 (Wild type)
147	2.3	G2	Negative	Preserved	Preserved	Preserved	Preserved	1.15 (Wild type)
148	2.4	G1	Positive	Preserved	Loss	Preserved	Preserved	0.97 (Wild type)
149	2.4	G1	Negative	Preserved	Preserved	Preserved	Preserved	1.04 (Wild type)
150	2.4	G1	Negative	Preserved	Preserved	Preserved	Preserved	0.97 (Wild type)
151	2.4	G1	Negative	Preserved	Preserved	Preserved	Preserved	1.00 (Wild type)
152	2.4	G1	Negative	Preserved	Preserved	Preserved	Preserved	0.97 (Wild type)
153	2.4	G1	Negative	Preserved	Preserved	Preserved	Preserved	1.19 (Wild type)
154	2.4	G1	Negative	Preserved	Preserved	Preserved	Preserved	1.16 (Wild type)
155	2.5	G1	Positive	Loss	Preserved	Preserved	Preserved	0.66 (Deletion)
156	2.5	G2	Positive	Preserved	Preserved	Preserved	Preserved	0.55 (Deletion)
157	2.5	G2	Negative	Preserved	Preserved	Preserved	Loss	0.46 (Deletion)
158	2.5	G1	Positive	Preserved	Loss	Loss	Preserved	1.00 (Wild type)
159	2.5	G2	Positive	Preserved	Loss	Preserved	Preserved	1.00 (Wild type)
160	2.5	G2	Positive	Loss	Loss	Preserved	Preserved	1.06 (Wild type)
161	2.5	G2	Positive	Loss	Loss	Preserved	Preserved	0.96 (Wild type)

162	2.5	G1	Negative	Preserved	Preserved	Preserved	Preserved	1.02 (Wild type)
163	2.5	G2	Negative	Preserved	Preserved	Preserved	Preserved	1.10 (Wild type)
164	2.5	G2	Negative	Preserved	Preserved	Preserved	Preserved	0.88 (Wild type)
165	2.5	G1	Negative	Preserved	Preserved	Preserved	Preserved	1.00 (Wild type)
166	2.5	G1	Negative	Preserved	Preserved	Preserved	Preserved	1.04 (Wild type)
167	2.5	G1	Negative	Preserved	Preserved	Preserved	Preserved	0.99 (Wild type)
168	2.5	G2	Negative	Preserved	Preserved	Preserved	Preserved	1.13 (Wild type)
169	2.5	G1	Negative	Preserved	Preserved	Preserved	Preserved	0.99 (Wild type)
170	2.5	G1	Negative	Preserved	Preserved	Preserved	Preserved	0.96 (Wild type)
171	2.5	G1	Negative	Preserved	Preserved	Preserved	Preserved	1.04 (Wild type)
172	2.5	G1	Negative	Preserved	Preserved	Preserved	Preserved	0.97 (Wild type)
173	2.5	G1	Negative	Preserved	Preserved	Preserved	Preserved	0.98 (Wild type)
174	2.5	G1	Negative	Preserved	Preserved	Preserved	Preserved	1.08 (Wild type)
175	2.5	G3	Negative	Preserved	Preserved	Preserved	Preserved	1.04 (Wild type)
176	2.6	G2	Negative	Preserved	Preserved	Preserved	Preserved	0.99 (Wild type)
177	2.7	G1	Negative	Preserved	Preserved	Loss	Preserved	0.67 (Deletion)
178	2.7	G1	Positive	Loss	Loss	Preserved	Preserved	0.96 (Wild type)
179	2.7	G1	Negative	Preserved	Preserved	Preserved	Preserved	0.96 (Wild type)
180	2.7	G1	Negative	Preserved	Preserved	Preserved	Preserved	1.00 (Wild type)
181	2.7	G1	Negative	Preserved	Preserved	Preserved	Preserved	1.19 (Wild type)
182	2.8	G1	Negative	Preserved	Preserved	Preserved	Preserved	0.59 (Deletion)
183	2.8	G2	Positive	Loss	Loss	Loss	Preserved	1.06 (Wild type)
184	2.8	G1	Positive	Loss	Preserved	Preserved	Preserved	1.01 (Wild type)
185	2.8	G1	Negative	Preserved	Preserved	Preserved	Preserved	1.00 (Wild type)
186	2.8	G1	Negative	Preserved	Preserved	Preserved	Preserved	1.00 (Wild type)
187	2.8	G1	Negative	Preserved	Preserved	Preserved	Preserved	0.99 (Wild type)
188	2.8	G1	Negative	Preserved	Preserved	Preserved	Preserved	1.00 (Wild type)
189	2.8	G1	Negative	Preserved	Preserved	Preserved	Preserved	1.00 (Wild type)
190	2.8	G1	Negative	Preserved	Preserved	Preserved	Preserved	1.00 (Wild type)
191	2.9	G1	Negative	Preserved	Preserved	Preserved	Preserved	1.05 (Wild type)
192	3.0	G2	Positive	Loss	Preserved	Preserved	Preserved	0.35 (Deletion)
193	3.0	G1	Negative	Preserved	Preserved	Preserved	Preserved	0.70 (Deletion)
194	3.0	G1	Negative	Preserved	Preserved	Preserved	Preserved	0.43 (Deletion)

195	3.0	G2	Positive	Loss	Loss	Loss	Preserved	1.11 (Wild type)
196	3.0	G2	Positive	Loss	Preserved	Preserved	Preserved	1.01 (Wild type)
197	3.0	G2	Positive	Preserved	Loss	Preserved	Preserved	1.00 (Wild type)
198	3.0	G1	Positive	Loss	Loss	Preserved	Preserved	1.01 (Wild type)
199	3.0	G2	Positive	Preserved	Preserved	Preserved	Preserved	0.99 (Wild type)
200	3.0	G2	Negative	Preserved	Preserved	Preserved	Preserved	1.08 (Wild type)
201	3.0	G2	Negative	Preserved	Preserved	Preserved	Preserved	1.00 (Wild type)
202	3.0	G2	Negative	Preserved	Preserved	Preserved	Preserved	0.89 (Wild type)
203	3.0	G1	Negative	Preserved	Preserved	Preserved	Preserved	0.99 (Wild type)
204	3.0	G1	Negative	Preserved	Preserved	Preserved	Preserved	0.96 (Wild type)
205	3.0	G1	Negative	Preserved	Preserved	Preserved	Preserved	1.06 (Wild type)
206	3.0	G2	Negative	Preserved	Preserved	Preserved	Preserved	1.00 (Wild type)
207	3.1	G1	Positive	Loss	Preserved	Preserved	Preserved	1.00 (Wild type)
208	3.1	G1	Negative	Preserved	Preserved	Preserved	Preserved	1.00 (Wild type)
209	3.2	G1	Positive	Loss	Preserved	Preserved	Preserved	1.11 (Wild type)
210	3.2	G1	Negative	Preserved	Preserved	Preserved	Preserved	0.92 (Wild type)
211	3.2	G1	Negative	Preserved	Preserved	Preserved	Preserved	1.01 (Wild type)
212	3.3	G1	Negative	Preserved	Preserved	Preserved	Preserved	0.84 (Wild type)
213	3.4	G2	Positive	Preserved	Preserved	Preserved	Preserved	1.02 (Wild type)
214	3.5	G1	Positive	Loss	Preserved	Loss	Preserved	0.65 (Deletion)
215	3.5	G1	Negative	Preserved	Preserved	Preserved	Preserved	0.74 (Deletion)
216	3.5	G1	Positive	Preserved	Loss	Preserved	Loss	1.02 (Wild type)
217	3.5	G2	Positive	Preserved	Loss	Loss	Preserved	0.97 (Wild type)
218	3.5	G2	Negative	Preserved	Preserved	Loss	Preserved	1.12 (Wild type)
219	3.5	G1	Negative	Preserved	Preserved	Loss	Preserved	0.99 (Wild type)
220	3.5	G1	Negative	Preserved	Preserved	Loss	Preserved	1.10 (Wild type)
221	3.5	G2	Positive	Loss	Loss	Preserved	Preserved	1.01 (Wild type)
222	3.5	G2	Positive	Preserved	Loss	Preserved	Preserved	1.00 (Wild type)
223	3.5	G2	Positive	Loss	Preserved	Preserved	Preserved	1.02 (Wild type)
224	3.5	G2	Positive	Loss	Preserved	Preserved	Preserved	1.14 (Wild type)
225	3.5	G1	Positive	Loss	Preserved	Preserved	Preserved	1.02 (Wild type)
226	3.5	G2	Positive	Loss	Preserved	Preserved	Preserved	1.19 (Wild type)
227	3.5	G1	Positive	Preserved	Preserved	Preserved	Preserved	0.98 (Wild type)

228	3.5	G1	Negative	Preserved	Preserved	Preserved	Preserved	1.07 (Wild type)
229	3.5	G2	Negative	Preserved	Preserved	Preserved	Preserved	1.06 (Wild type)
230	3.5	G1	Negative	Preserved	Preserved	Preserved	Preserved	1.01 (Wild type)
231	3.5	G1	Negative	Preserved	Preserved	Preserved	Preserved	0.97 (Wild type)
232	3.6	G2	Negative	Preserved	Preserved	Preserved	Preserved	0.97 (Wild type)
233	3.6	G1	Negative	Preserved	Preserved	Preserved	Preserved	0.95 (Wild type)
234	3.6	G2	Negative	Preserved	Preserved	Preserved	Preserved	1.03 (Wild type)
235	3.7	G1	Positive	Loss	Preserved	Preserved	Preserved	0.65 (Deletion)
236	3.7	G3	Positive	Preserved	Loss	Preserved	Preserved	0.97 (Wild type)
237	3.8	G2	Positive	Preserved	Loss	Preserved	Preserved	0.97 (Wild type)
238	3.8	G1	Negative	Preserved	Preserved	Preserved	Preserved	0.99 (Wild type)
239	3.8	G1	Negative	Preserved	Preserved	Preserved	Preserved	1.09 (Wild type)
240	4.0	G1	Positive	Preserved	Loss	Loss	Preserved	0.98 (Wild type)
241	4.0	G1	Positive	Preserved	Preserved	Loss	Preserved	1.08 (Wild type)
242	4.0	G2	Negative	Preserved	Preserved	Preserved	Loss	1.06 (Wild type)
243	4.0	G1	Positive	Preserved	Loss	Preserved	Preserved	1.08 (Wild type)
244	4.0	G2	Positive	Preserved	Loss	Preserved	Preserved	0.97 (Wild type)
245	4.0	G2	Positive	Preserved	Loss	Preserved	Preserved	0.85 (Wild type)
246	4.0	G2	Negative	Preserved	Preserved	Preserved	Preserved	1.02 (Wild type)
247	4.0	G2	Negative	Preserved	Preserved	Preserved	Preserved	0.92 (Wild type)
248	4.0	G1	Negative	Preserved	Preserved	Preserved	Preserved	0.90 (Wild type)
249	4.0	G2	Negative	Preserved	Preserved	Preserved	Preserved	1.06 (Wild type)
250	4.0	G2	Negative	Preserved	Preserved	Preserved	Preserved	1.17 (Wild type)
251	4.0	G2	Negative	Preserved	Preserved	Preserved	Preserved	0.97 (Wild type)
252	4.0	G2	Negative	Preserved	Preserved	Preserved	Preserved	0.89 (Wild type)
253	4.0	G2	Negative	Preserved	Preserved	Preserved	Preserved	1.03 (Wild type)
254	4.2	G2	Positive	Loss	Loss	Preserved	Preserved	0.29 (Deletion)
255	4.2	G1	Negative	Preserved	Preserved	Preserved	Preserved	1.03 (Wild type)
256	4.2	G1	Negative	Preserved	Preserved	Preserved	Preserved	0.99 (Wild type)
257	4.2	G3	Negative	Preserved	Preserved	Preserved	Preserved	0.99 (Wild type)
258	4.2	G2	Negative	Preserved	Preserved	Preserved	Preserved	0.98 (Wild type)
259	4.4	G1	Negative	Preserved	Preserved	Preserved	Preserved	1.04 (Wild type)
260	4.5	G3	Negative	Preserved	Preserved	Preserved	Preserved	0.67 (Deletion)

261	4.5	G2	Negative	Preserved	Preserved	Preserved	Loss	0.53 (Deletion)
262	4.5	G2	Positive	Loss	Preserved	Loss	Preserved	0.96 (Wild type)
263	4.5	G3	Negative	Preserved	Preserved	Preserved	Loss	1.01 (Wild type)
264	4.5	G2	Positive	Loss	Preserved	Preserved	Preserved	0.93 (Wild type)
265	4.5	G2	Positive	Preserved	Loss	Preserved	Preserved	0.98 (Wild type)
266	4.5	G2	Positive	Preserved	Loss	Preserved	Preserved	0.99 (Wild type)
267	4.5	G1	Negative	Preserved	Preserved	Preserved	Preserved	0.95 (Wild type)
268	4.5	G1	Negative	Preserved	Preserved	Preserved	Preserved	0.97 (Wild type)
269	4.5	G1	Negative	Preserved	Preserved	Preserved	Preserved	0.96 (Wild type)
270	4.5	G1	Negative	Preserved	Preserved	Preserved	Preserved	0.99 (Wild type)
271	4.5	G1	Negative	Preserved	Preserved	Preserved	Preserved	0.99 (Wild type)
272	4.5	G2	Negative	Preserved	Preserved	Preserved	Preserved	0.86 (Wild type)
273	4.6	G2	Positive	Preserved	Preserved	Preserved	Preserved	0.99 (Wild type)
274	4.6	G2	Negative	Preserved	Preserved	Preserved	Preserved	0.98 (Wild type)
275	4.6	G2	Negative	Preserved	Preserved	Preserved	Preserved	0.99 (Wild type)
276	4.8	G1	Positive	Loss	Loss	Preserved	Preserved	0.97 (Wild type)
277	4.9	G2	Positive	Preserved	Loss	Preserved	Preserved	0.69 (Deletion)
278	5.0	G2	Negative	Preserved	Preserved	Loss	Preserved	1.01 (Wild type)
279	5.0	G2	Positive	Preserved	Loss	Preserved	Preserved	1.00 (Wild type)
280	5.0	G2	Negative	Preserved	Preserved	Preserved	Preserved	1.01 (Wild type)
281	5.0	G3	Negative	Preserved	Preserved	Preserved	Preserved	1.01 (Wild type)
282	5.0	G1	Negative	Preserved	Preserved	Preserved	Preserved	0.96 (Wild type)
283	5.0	G1	Negative	Preserved	Preserved	Preserved	Preserved	1.00 (Wild type)
284	5.1	G1	Negative	Preserved	Preserved	Preserved	Preserved	0.96 (Wild type)
285	5.3	G2	Positive	Preserved	Loss	Preserved	Preserved	1.03 (Wild type)
286	5.5	G2	Positive	Loss	Preserved	Preserved	Preserved	0.95 (Wild type)
287	5.5	G2	Positive	Loss	Loss	Preserved	Preserved	0.97 (Wild type)
288	5.5	G2	Positive	Preserved	Loss	Preserved	Preserved	0.99 (Wild type)
289	5.5	G2	Positive	Preserved	Loss	Preserved	Preserved	0.99 (Wild type)
290	5.5	G2	Negative	Preserved	Preserved	Preserved	Preserved	0.88 (Wild type)
291	5.6	G2	Positive	Loss	Preserved	Preserved	Preserved	1.01 (Wild type)
292	5.7	G1	Positive	Loss	Preserved	Preserved	Preserved	0.95 (Wild type)
293	5.8	G1	Positive	Preserved	Preserved	Preserved	Preserved	0.90 (Wild type)

294	6.0	G2	Positive	Preserved	Loss	Preserved	Preserved	0.77 (Deletion)
295	6.0	G2	Negative	Preserved	Preserved	Preserved	Loss	0.95 (Wild type)
296	6.0	G2	Negative	Preserved	Preserved	Loss	Preserved	1.00 (Wild type)
297	6.0	G2	Negative	Preserved	Preserved	Loss	Preserved	1.00 (Wild type)
298	6.0	G2	Negative	Preserved	Preserved	Loss	Preserved	0.89 (Wild type)
299	6.0	G2	Positive	Preserved	Loss	Preserved	Preserved	0.97 (Wild type)
300	6.0	G2	Positive	Loss	Preserved	Preserved	Preserved	0.98 (Wild type)
301	6.0	G1	Positive	Loss	Preserved	Preserved	Preserved	1.02 (Wild type)
302	6.0	G2	Positive	Preserved	Loss	Preserved	Preserved	0.99 (Wild type)
303	6.0	G1	Positive	Preserved	Loss	Preserved	Preserved	0.96 (Wild type)
304	6.0	G2	Negative	Preserved	Preserved	Preserved	Preserved	0.96 (Wild type)
305	6.0	G1	Negative	Preserved	Preserved	Preserved	Preserved	0.94 (Wild type)
306	6.0	G2	Negative	Preserved	Preserved	Preserved	Preserved	0.84 (Wild type)
307	6.4	G2	Negative	Preserved	Preserved	Loss	Preserved	0.48 (Deletion)
308	6.5	G3	Positive	Loss	Loss	Preserved	Preserved	0.66 (Deletion)
309	6.5	G2	Positive	Preserved	Loss	Loss	Preserved	0.98 (Wild type)
310	6.5	G2	Negative	Preserved	Preserved	Preserved	Preserved	1.03 (Wild type)
311	6.5	G2	Negative	Preserved	Preserved	Preserved	Preserved	1.00 (Wild type)
312	6.5	G2	Negative	Preserved	Preserved	Preserved	Preserved	0.91 (Wild type)
313	6.8	G2	Positive	Preserved	Loss	Preserved	Preserved	0.98 (Wild type)
314	7.0	G2	Positive	Preserved	Loss	Preserved	Preserved	1.01 (Wild type)
315	7.0	G1	Positive	Loss	Preserved	Preserved	Preserved	0.93 (Wild type)
316	7.0	G2	Positive	Loss	Preserved	Preserved	Preserved	0.95 (Wild type)
317	7.0	G1	Negative	Preserved	Preserved	Preserved	Preserved	0.97 (Wild type)
318	7.0	G2	Negative	Preserved	Preserved	Preserved	Preserved	0.98 (Wild type)
319	7.0	G2	Negative	Preserved	Preserved	Preserved	Preserved	0.92 (Wild type)
320	7.5	G2	Positive	Preserved	Loss	Preserved	Preserved	0.24 (Deletion)
321	7.5	G2	Positive	Preserved	Preserved	Preserved	Preserved	0.72 (Deletion)
322	7.5	G2	Positive	Preserved	Loss	Preserved	Loss	0.97 (Wild type)
323	7.5	G2	Positive	Preserved	Preserved	Preserved	Preserved	0.98 (Wild type)
324	7.5	G2	Negative	Preserved	Preserved	Preserved	Preserved	1.00 (Wild type)
325	7.5	G1	Negative	Preserved	Preserved	Preserved	Preserved	0.95 (Wild type)
326	7.5	G1	Negative	Preserved	Preserved	Preserved	Preserved	0.95 (Wild type)

327	8.0	G2	Positive	Preserved	Loss	Preserved	Preserved	0.88 (Wild type)
328	8.5	G2	Negative	Preserved	Preserved	Loss	Preserved	1.01 (Wild type)
329	8.5	G2	Positive	Loss	Preserved	Preserved	Preserved	0.95 (Wild type)
330	8.5	G2	Negative	Preserved	Preserved	Preserved	Preserved	0.97 (Wild type)
331	9.0	G2	Positive	Loss	Loss	Loss	Preserved	0.99 (Wild type)
332	9.0	G3	Positive	Preserved	Preserved	Loss	Preserved	0.84 (Wild type)
333	9.0	G1	Negative	Preserved	Preserved	Preserved	Loss	0.95 (Wild type)
334	9.0	G1	Negative	Preserved	Preserved	Preserved	Preserved	0.98 (Wild type)
335	9.5	G2	Positive	Preserved	Preserved	Loss	Preserved	0.88 (Wild type)
336	10.0	G2	Positive	Preserved	Loss	Preserved	Preserved	0.56 (Deletion)
337	10.0	G2	Positive	Preserved	Preserved	Preserved	Preserved	0.53 (Deletion)
338	10.0	G2	Positive	Loss	Preserved	Loss	Preserved	0.94 (Wild type)
339	10.0	G1	Negative	Preserved	Preserved	Preserved	Preserved	0.96 (Wild type)
340	10.0	G2	Negative	Preserved	Preserved	Preserved	Preserved	0.99 (Wild type)
341	12.0	G2	Positive	Loss	Preserved	Preserved	Preserved	1.00 (Wild type)
342	12.2	G2	Positive	Preserved	Loss	Preserved	Preserved	0.96 (Wild type)
343	14.0	G1	Positive	Preserved	Loss	Preserved	Preserved	0.19 (Deletion)
344	15.0	G2	Positive	Loss	Preserved	Preserved	Preserved	0.95 (Wild type)
345	15.0	G2	Positive	Loss	Preserved	Preserved	Preserved	0.95 (Wild type)
346	17.0	G2	Negative	Preserved	Preserved	Preserved	Loss	0.94 (Wild type)
347	18.0	G2	Positive	Preserved	Preserved	Loss	Preserved	0.93 (Wild type)

Abbreviations: ALT, alternative lengthening of telomeres

Supplementary Table 3. Clinical and pathologic comparison of DAXX/ATRX, H3K36me3, ARID1A and CDKN2A status in non-syndromic well-differentiated PanNETs.

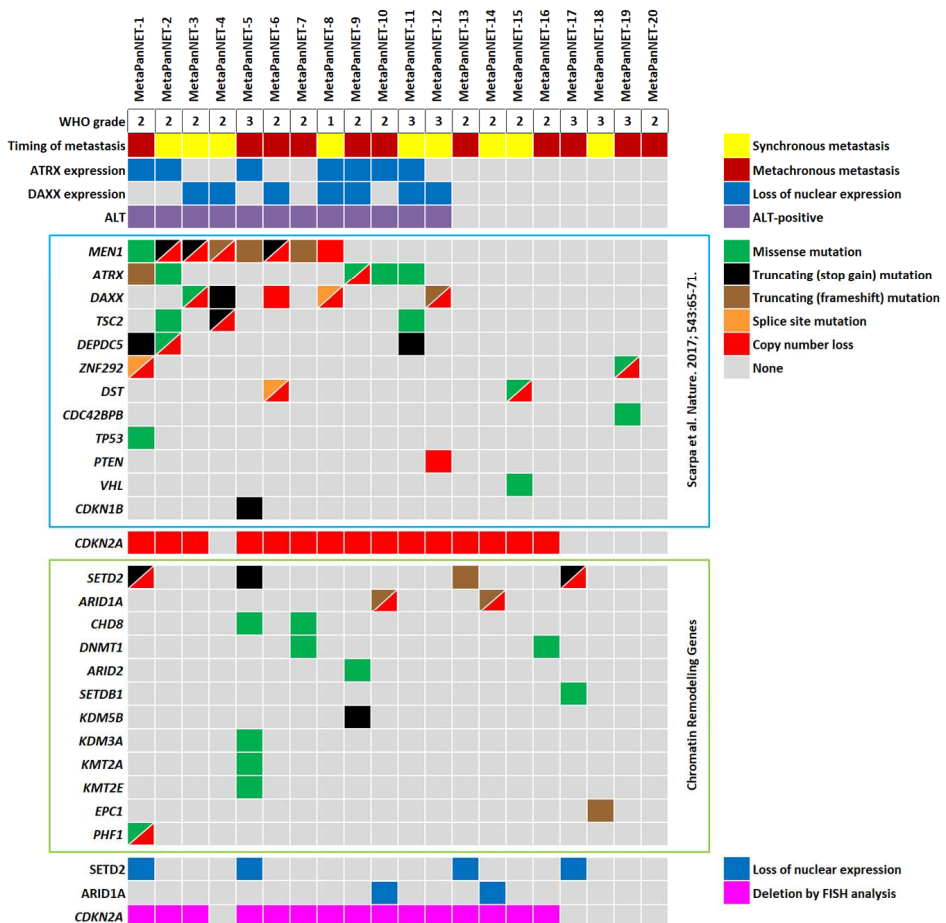
Patient or Tumor Characteristics	DAXX/ATRX			H3K36me3			ARID1A			CDKN2A		DAXX/ATRX/H3K36me3/ARID1A/CDKN2A		p	
	Preserved	Loss	p	Preserved	Loss	p	Preserved	Loss	p	Wildtype	Deletion	p	Preserved/Wildtype	Loss/Deletion	
Gender															
Female	139 (84%)	27 (16%)	0.005	155 (93%)	11 (7%)	0.431	161 (97%)	5 (3%)	1.000	154 (93%)	12 (7%)	1.000	124 (75%)	42 (25%)	0.008
Male	128 (71%)	53 (29%)		164 (91%)	17 (9%)		176 (97%)	5 (3%)		168 (93%)	13 (7%)		111 (61%)	70 (39%)	
Mean age (range), years	58.3 (26 - 85)	61.3 (31 - 83)	0.057	59.1 (26 - 85)	57.6 (32 - 82)	0.546	59.1 (26 - 83)	57.3 (37 - 85)	0.679	58.8 (26 - 85)	61.8 (37 - 80)	0.241	58.4 (26 - 83)	60.4 (31 - 85)	0.162
Mean tumor size (range), cm	3.0 (0.6 - 18.0)	5.0 (1.0 - 15.0)	< 0.001	3.3 (0.6 - 17.0)	5.3 (1.2 - 18.0)	< 0.001	3.3 (0.6 - 18.0)	6.0 (1.7 - 17.0)	0.002	3.3 (0.6 - 18.0)	4.9 (2.0 - 14.0)	0.004	2.6 (0.6 - 10.0)	5.2 (1.0 - 18.0)	< 0.001
Functional*	33 (92%)	3 (8%)	0.034	36 (100%)	0 (0%)	0.096	36 (100%)	0 (0%)	0.607	36 (100%)	0 (0%)	0.091	33 (92%)	3 (8%)	0.001
Insulinoma	21 (100%)	0 (0%)		21 (100%)	0 (0%)		21 (100%)	0 (0%)		21 (100%)	0 (0%)		21 (100%)	0 (0%)	
Gastrinoma	7 (88%)	1 (12%)		8 (100%)	0 (0%)		8 (100%)	0 (0%)		8 (100%)	0 (0%)		7 (88%)	1 (12%)	
Glucagonoma	4 (100%)	0 (0%)		4 (100%)	0 (0%)		4 (100%)	0 (0%)		4 (100%)	0 (0%)		4 (100%)	0 (0%)	
Somatostatinoma	0 (0%)	1 (100%)		1 (100%)	0 (0%)		1 (100%)	0 (0%)		1 (100%)	0 (0%)		0 (0%)	1 (100%)	
VIPoma	1 (100%)	0 (0%)		1 (100%)	0 (0%)		1 (100%)	0 (0%)		1 (100%)	0 (0%)		1 (100%)	0 (0%)	
ACTH-producing	0 (0%)	1 (100%)		1 (100%)	0 (0%)		1 (100%)	0 (0%)		1 (100%)	0 (0%)		0 (0%)	1 (100%)	
Location															
Head and uncinate	104 (79%)	27 (21%)	0.432	113 (86%)	18 (14%)	0.004	128 (98%)	3 (2%)	0.748	120 (92%)	11 (8%)	0.526	88 (67%)	43 (33%)	0.906
Body and tail	163 (75%)	53 (25%)		206 (95%)	10 (5%)		209 (97%)	7 (3%)		202 (94%)	14 (6%)		147 (68%)	69 (32%)	
WHO grade															
Low (G1)	175 (88%)	24 (12%)	< 0.001	191 (96%)	8 (4%)	0.004	197 (99%)	2 (1%)	0.026	190 (95%)	9 (5%)	0.033	165 (83%)	34 (17%)	< 0.001
Intermediate (G2)	86 (61%)	54 (39%)		121 (86%)	19 (14%)		133 (95%)	7 (5%)		126 (90%)	14 (10%)		67 (48%)	73 (52%)	
High (G3)	6 (75%)	2 (25%)		7 (88%)	1 (12%)		7 (88%)	1 (12%)		6 (75%)	2 (25%)		3 (38%)	5 (62%)	
Lymphovascular invasion	93 (61%)	60 (39%)	< 0.001	133 (87%)	20 (13%)	0.003	143 (93%)	10 (7%)	< 0.001	131 (86%)	22 (14%)	< 0.001	67 (44%)	86 (56%)	< 0.001
Perineural invasion	59 (65%)	32 (25%)	0.002	77 (85%)	14 (15%)	0.006	86 (95%)	5 (5%)	0.136	78 (86%)	13 (14%)	0.004	42 (46%)	49 (54%)	< 0.001
Primary tumor (pT) stage															
T1	115 (95%)	6 (5%)	< 0.001	118 (98%)	3 (2%)	0.001	120 (99%)	1 (1%)	0.001	120 (99%)	1 (1%)	< 0.001	113 (93%)	8 (7%)	< 0.001
T2	80 (75%)	26 (25%)		99 (93%)	7 (7%)		106 (100%)	0 (0%)		99 (93%)	7 (7%)		74 (70%)	32 (30%)	
T3	72 (60%)	48 (40%)		102 (85%)	18 (15%)		111 (93%)	9 (7%)		103 (86%)	17 (14%)		48 (40%)	72 (60%)	
Lymph node metastases (n = 294)**	62 (56%)	48 (44%)	< 0.001	98 (89%)	12 (11%)	0.397	103 (94%)	7 (6%)	0.044	94 (85%)	16 (15%)	0.003	45 (41%)	65 (59%)	< 0.001
Synchronous metastases	28 (51%)	27 (49%)	< 0.001	44 (80%)	11 (20%)	0.002	50 (91%)	5 (9%)	0.011	45 (82%)	10 (18%)	0.002	14 (25%)	41 (75%)	< 0.001
Metachronous metastases (n = 282)***	17 (38%)	28 (62%)	< 0.001	36 (80%)	9 (20%)	< 0.001	42 (93%)	3 (7%)	0.027	33 (73%)	12 (27%)	< 0.001	5 (11%)	40 (89%)	< 0.001
Presence of ALT (n = 94)	14 (15%)	80 (85%)	< 0.001	79 (84%)	15 (16%)	0.003	91 (97%)	3 (3%)	0.734	78 (83%)	16 (17%)	< 0.001	7 (7%)	87 (93%)	< 0.001
Loss of DAXX/ATRX (n = 80)				69 (86%)	11 (14%)	0.058	77 (96%)	3 (4%)	0.702	67 (84%)	13 (16%)	0.001			
Loss of H3K36me3 (n = 28)	17 (61%)	11 (39%)	0.058				28 (100%)	0 (0%)	1.000	25 (89%)	3 (11%)	0.440			
Loss of ARID1A (n = 10)	7 (70%)	3 (30%)	0.702	10 (100%)	0 (0%)	1.000				8 (80%)	2 (20%)	0.157			
Deletion in CDKN2A (n = 25)	12 (48%)	13 (52%)	0.001	22 (88%)	3 (12%)	0.440	23 (92%)	2 (8%)	0.157						

Abbreviations: ALT, alternative lengthening of telomeres

*Statistical analysis as reported is based on the presence or absence of functionality and not functional subtype.

**Regional lymph nodes were present for evaluation in 294 cases.

***The presence of metachronous metastasis was evaluated in patients that had not presented with synchronous metastases (n = 282).

A**B**